Heliyon 9 (2023) e14279

Contents lists available at ScienceDirect

Heliyon

journal homepage: www.cell.com/heliyon

Review article

Recent advances in density functional theory approach for optoelectronics properties of graphene

A.L. Olatomiwa [a,b,*], Tijjani Adam [a,b,c,**], C.O. Edet [b,d,e], A.A. Adewale [f], Abdullah Chik [g,h], Mohammed Mohammed [h,i], Subash C.B. Gopinath [a,c,h], U. Hashim [a]

[a] Institute of Nano Electronic Engineering, Universiti Malaysia Perlis, 01000, Kangar, Perlis, Malaysia
[b] Faculty of Electronic Engineering and Technology, Universiti Malaysia Perlis, 02600, Arau, Perlis, Malaysia
[c] Micro System Technology, Centre of Excellence (CoE), Universiti Malaysia Perlis (UniMAP), Pauh Campus, 02600, Arau, Perlis, Malaysia
[d] Institute of Engineering Mathematics, Universiti Malaysia Perlis, 02600, Arau, Perlis, Malaysia
[e] Department of Physics, Cross River University of Technology, Calabar, Nigeria
[f] Department of Pure and Applied Physics, Ladoke Akintola University of Technology, Ogbomoso, Nigeria
[g] Centre for Frontier Materials Research, Universiti Malaysia Perlis, 01000, Kangar, Perlis, Malaysia
[h] Faculty of Chemical Engineering and Technology, Universiti Malaysia Perlis (UniMAP), Taman Muhibbah, Jejawi, 02600, Arau, Perlis, Malaysia
[i] Center of Excellence Geopolymer & Green Technology (CEGeoGTech), Universiti Malaysia Perlis, 02600, Arau, Perlis, Malaysia

ARTICLE INFO

Keywords:
Graphene
Electronic
Optical properties
Thermal conductivities
Correlation functionals
QHE
Optoelectronics
ML-DFT
Descriptors
ML potentials
First Principles calculation

ABSTRACT

Graphene has received tremendous attention among diverse 2D materials because of its remarkable properties. Its emergence over the last two decades gave a new and distinct dynamic to the study of materials, with several research projects focusing on exploiting its intrinsic properties for optoelectronic devices. This review provides a comprehensive overview of several published articles based on density functional theory and recently introduced machine learning approaches applied to study the electronic and optical properties of graphene. A comprehensive catalogue of the bond lengths, band gaps, and formation energies of various doped graphene systems that determine thermodynamic stability was reported in the literature. In these studies, the peculiarity of the obtained results reported is consequent on the nature and type of the dopants, the choice of the XC functionals, the basis set, and the wrong input parameters. The different density functional theory models, as well as the strengths and uncertainties of the ML potentials employed in the machine learning approach to enhance the prediction models for graphene, were elucidated. Lastly, the thermal properties, modelling of graphene hetero-structures, the superconducting behaviour of graphene, and optimization of the DFT models are grey areas that future studies should explore in enhancing its unique potential. Therefore, the identified future trends and knowledge gaps have a prospect in both academia and industry to design future and reliable optoelectronic devices.

* Corresponding author. Institute of Nano Electronic Engineering, Universiti Malaysia Perlis, 01000, Perlis, Malaysia.
** Corresponding author. Faculty of Electronic Engineering and Technology, Universiti Malaysia Perlis, 02600, Arau, Perlis, Malaysia.
E-mail addresses: olatomiwa@studentmail.unimap.edu.my (A.L. Olatomiwa), tijjani@unimap.edu.my (T. Adam).

https://doi.org/10.1016/j.heliyon.2023.e14279
Received 8 December 2022; Received in revised form 28 February 2023; Accepted 1 March 2023
Available online 7 March 2023

1. Introduction

Almost every facet of our civilization is governed by the continual discovery of novel materials with specified functions and performances [1–3]. Today, the computational density functional theory technique has substantially expanded the materials design process, either alone or in tandem with experimental research, owing to the relatively complex level of concepts and computer modelling [1–3]. Moreover, at the turn of the last decade, graphene, a single layer of graphite exfoliated by Geim and co-workers, became the focus of intense research due to its remarkable physical properties [4–6]. Since its discovery, several 2D materials have been synthesized, including hexagonal boron nitride, silicene, transition metal dichalcogenide, antimonene, and phosphorene [7–11]. The properties of these materials are markedly different from those of the parent compound due to changes in the size of the crystal structure and quantum confinement [12,13].

Despite the surge in 2D materials, graphene stands out among them for having exceptional electronic, optical, and thermal properties [14,15]. It has very high carrier mobilities ($\sim$200,000 $cm^2V^{-1}S^{-1}$) [16–18], unusual linear dispersion around the Dirac point [19,20], ultrahigh thermal conductivities ($\sim$ 5000 W/mk) [21–23], room temperature ballistic carrier transport [24,25], large surface area (2630 m^2/g) [26–28], a Young's Modulus of 1 TPa [29,30], broadband optical absorbance (2.3%) [31–33], and a robust crystal structure, all of which reveal the material's high quality and suggest its prospects for future optoelectronic devices [34–36]. However, its use in optoelectronics is limited due to its zero bandgap and relatively poor structural tunability [37–39]. Therefore, several reports have established different approaches to induce a sizeable band gap and efficiently modulate the intrinsic properties of graphene by stacking configuration, mechanical strain, electric and magnetic fields, and heteroatom chemical doping via DFT methods for next-generation electronics with designer functionalities [40–42].

In this paper, we present an extensive review of heteroatom doping of graphene employing the DFT within the last decade as well as the recently introduced data-driven ML-DFT models because these are regarded as the most effective method of manipulating the properties of graphene [43–45]. Moreover, these modifications in the properties of graphene are largely determined by the types of dopant atoms, their percentages, and the doping sites [42]. Additionally, these heteroatoms can either be electron acceptor (p-type) or electron donor (n-type) systems when substituted into graphene, depending on the number of valence electrons in the dopant atom [46–48]. Therefore, a comprehensive catalogue of the methods and results will provide insights into the achievements, present status, and shortfalls in the research area. To that end, in Section 2.1, we present an overview of the heritage of graphene as well as an in-depth review of the electronic and optical properties calculated using the density functional approach. Section 3.1 is dedicated to the models and implementation platforms for both traditional DFT and ML-DFT for the electronic structure calculation of graphene. Lastly, this section is concluded by revealing some knowledge gaps and future trends in the literature on the study of graphene. Section 4 presents a concluding remark.

2. Overview of the heritage of graphene and selected properties

Graphene has remained the "*de facto*" and most studied 2D material for almost two decades, with its discovery changing the dynamics of the materials world [49,50]. In 2013, about two scientific articles on the application of graphene were published every 96 min, which was over forty journals every 24 h [51]. Interestingly, graphene research has further advanced, Fig. 1(a–b) reveals the status of the globally published related material and graphene research publication per year from 2010 to 2021.

More broadly, graphene is the first of a large family tree of 2D nanomaterials as shown in Fig. 2 which includes a plethora of different carbon materials ranging from fullerenes (0D), carbon nanotubes (1D), graphene oxide (GO) to graphene quantum dots (GQDs), and other derivatives introducing physics for low-dimensional systems which have never ceased to amaze, proving to usher in

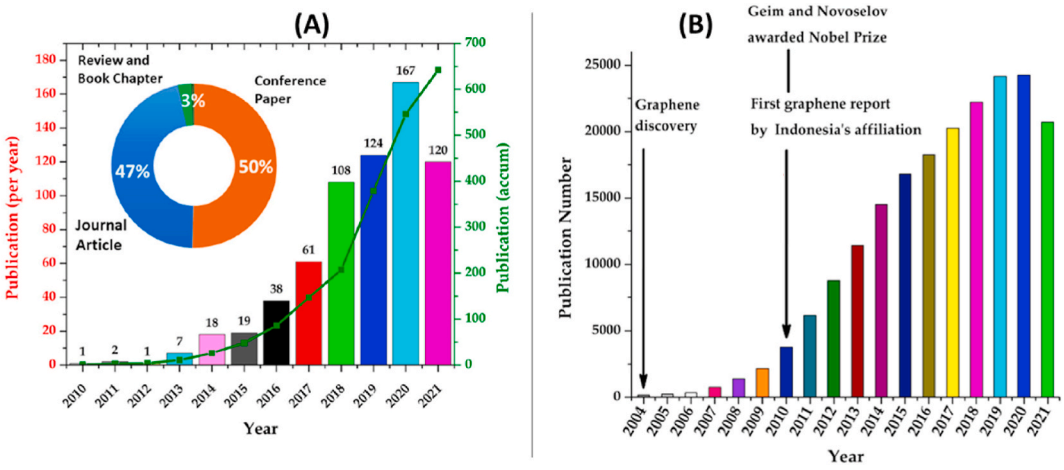

Fig. 1. Fig. 1: (a) The Schematic illustration of Graphene's globally published research articles from 2004 to 2021 and (b) graphene's related publications from 2004 to 2021. Figure remodified from Ref. [52].

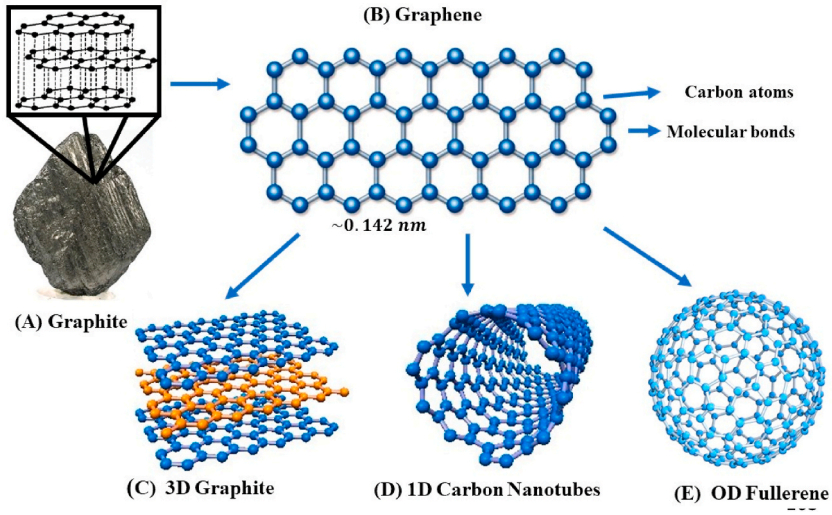

Fig. 2. The Schematic illustration of the Origin and the transformation of graphite to graphene's atomic structure. The transformation process shows that graphene, a 2D basic unit of carbon can be folded into (C) 3-D Graphite (D) rolled into 1-D nanotubes (E) and folded into 0-D Fullerene. Figure remodified from Ref. [80].

a new generation system [53]. The earliest evidence of graphene was reported when Benjamin Brodie created carbonic acid in the second millennium, which he hypothesized was a new form of carbon and proposed the name "graphon". In the ensuing century, only a few studies have described the layered structure of graphite oxide, which was shown to contain distinct atomic planes [54]. The discovery of graphite oxide paper was reported by Kohlschutter and Haenni [55,56] and subsequently, in the mid-'90s, Ruess and Vogt [57] employed a transmission electron microscope to observe graphite oxide flakes with a thickness of a few nanometers that were produced by the evaporation of a suspension droplet placed on the TEM grid [55,56]. Meanwhile, Boehm et al. [58] initiated the chemical method of reducing graphite oxide in a diluted alkaline solution of hydrazine and hydrogen sulphide under proper conditions a few years later and subsequently proposed the term "graphene" in the late twentieth century to designate a variety of carbon-based compounds, which enables the isolation of mono and few layers graphitic layers [58,59]. However, Wallace [60] was the first to propose graphene as a theoretical construct to aid in the calculation of graphite's band structure [61]. Moreover, a decade earlier, it was demonstrated that a 2D crystal could not exist because the system was not in equilibrium [62]. The idea was later expanded with a plethora of experimental evidence [62,63]. It was not until nineteen years ago that a successful method for separating graphene from graphite by mechanical exfoliation with scotch tape was discovered in Manchester [64,65]. This discovery sparked widespread interest in graphene, and numerous experts around the world have since conducted extensive research on this ubiquitous material [66]. Its large honeycomb network serves as the foundation for several other allotropes, as displayed in Fig. 2(a)–(e). This one-atom-thick layer of graphite called graphene demonstrates an extremely strong absorption for a monolayer atom that is wavelength-independent [39]. However, graphene has a gapless band structure, and the total absorption and quantum efficiency are still poor. Therefore, for graphene to realize its potential a sizeable band gap must be created to enhance the optical properties for application in electronic devices with optimized stability and performance while widening the scope for novel electronic designs [67–71].

2.1. The structural properties of pure graphene material

Graphene is a remarkably 2D layer with a C–C bond length of 1.420 Å, as displayed in Fig. 2b, (the simplest and most important crystalline allotrope of carbon atoms), which originates in a tightly packed hexagonal lattice with a purely sp2 orbital hybridization at ambient temperature [72,73]. This σ bond results in some impressive mechanical properties [74]. A three-sided network with a two-atom basis for each cell makes up the structure. The graphene lattice vectors in Eq. (1) are expressed as follows [69]:

$$a_1 = \frac{a}{2}\left(3, \sqrt{3}\right), a_2 = \frac{a}{2}\left(3, -\sqrt{3}\right) \tag{1}$$

The distance between near-set neighbor atoms is expressed as $a = 1.42$Å. The vectors of the reciprocal-lattice in Eq. (2) are determined by:

$$b_1 = \frac{2\pi}{3a}\left(1, \sqrt{3}\right), b_2 = \frac{2\pi}{3a}\left(1, -\sqrt{3}\right) \tag{2}$$

The sp^2 hybridization consists of orbitals from the S, P_x and P_z families. In the hexagonal phase, three different carbon atoms form covalent bonds with one other, leaving one free electron for each carbon atom. This free electron is held in the P_z orbital, which is above the plane and creates the π bond. Moreover, the exceptional properties of this 2D nanomaterial rely heavily on this free radical [75,76]. The half-filled π band allows the highly mobile non-bonding electrons to travel easily in graphene. Therefore, the π -band

reduces at half-filling to two inequivalent locations at the corners of the first Brillouin zone, resulting in Dirac cones [77]. Furthermore, in the bilayer and multilayer graphene, the π-bonds produce a van der Waals interconnection with the layers of graphene [78,79].

2.2. The electronic properties of pure graphene

The tight-binding method was employed by Wallace in investigating the electronic band structure of a monolayer of graphite [60, 81,82]. And subsequently, Castro Neto and others have also reported graphene's electronic properties and discussed how these properties are determined by stacking graphene layers [69,83]. Thus, graphene has drawn so much research interest for optoelectronic applications due to its high electron mobilities (15,000 cm^2/V) at room temperature and unusual electronic behaviours such as the quantum hall effect (QHE), which mimics massless transportation, leading to its high superconductivity [84]. The QHE is further discussed later in this section. Moreover, it's worth noting that structural holes allow phonons to pass through unhindered, resulting in high thermal conductivity in graphene. Additionally, graphene displays a semi-metallic behaviour; the band structure reveals the unoccupied (π*) and occupied (π) bands overlap at the same K point just below the Fermi energy level with linear dispersion near it. In addition, the density of states contains the valence and conduction bands, with a disappearing density at the Fermi level, which is mostly generated by π states, as displayed in Fig. 4(c) [85–87]. Moreover, the schematic illustration of the formation process based on the basic elements of graphene's bonding properties, the honeycomb structure, the SEM image of graphene's single layer and the calculated band structure of graphene is displayed in Fig. 3(a–f).

Furthermore, the upper side of the linear dispersion curve shown in Fig. 3(f), describes the π* (upper conduction) energy anti-bonding band, and the bottom side, which defines the energy bonding band. At the Dirac point k, the π* and π band are reduced, indicating that pure graphene is a two-dimensional gapless semimetal [88]. The charge carriers in graphene are generally defined by the Dirac equation and not the Schrodinger equation due to the uniformity of the crystal lattice, which comprises two identical carbon sublattices A and B.

Moreso, the electronic sub-bands consisting of a mixture of equal and unequal wave functions for the two sublattices overlap at the Brillouin zone's edge, giving rise to a cone shape around the Dirac point describing the electron dynamics as the energy and the quasi momentum lies in the same plane i.e., the dispersion relationship in metals and semiconductors is shaped like a parabola as displayed in Fig. 4(a) and (b) [89]. The Dirac points at the edge of the graphene Brillouin zone are very critical for the graphene physics as displayed in Fig. 4(a). The placements of these objects in momentum space are determined by Eq. (3) [90].

$$K = \left(\frac{2\pi}{3a_1}, \frac{2\pi}{5.196\,a_1}\right), K' = \left(\frac{2\pi}{3a}, -\frac{2\pi}{5.196a_1}\right) \tag{3}$$

The three nearest-neighbor vectors in Eq. (4) are expressed as follows in real space:

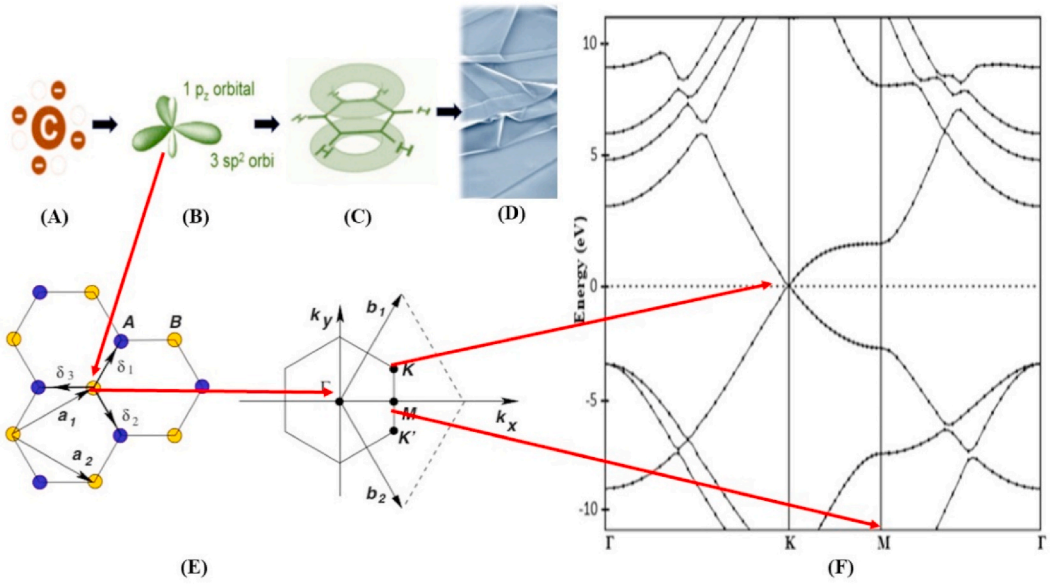

Fig. 3. (a–c) Schematic illustration of the formation process from the basic element of graphene bonding properties and (d) the mono-layer graphene SEM image (e) the honeycomb lattice and its Brillouin zones. The L.H.S. reveals the interpenetrating triangular lattices that make up the lattice structure of 2D graphene. The vectors of the closest neighbors are represented by $\delta_{i,} = 1, 2, 3$ and a_1 and a_2 unit is the lattices respectively. The R.H.S reveals the Dirac Cone which is created by the valence and conduction band crossing at the K and K' point This is indicated in (f) the band structure of pure graphene. Figure remodified from Ref. [88].

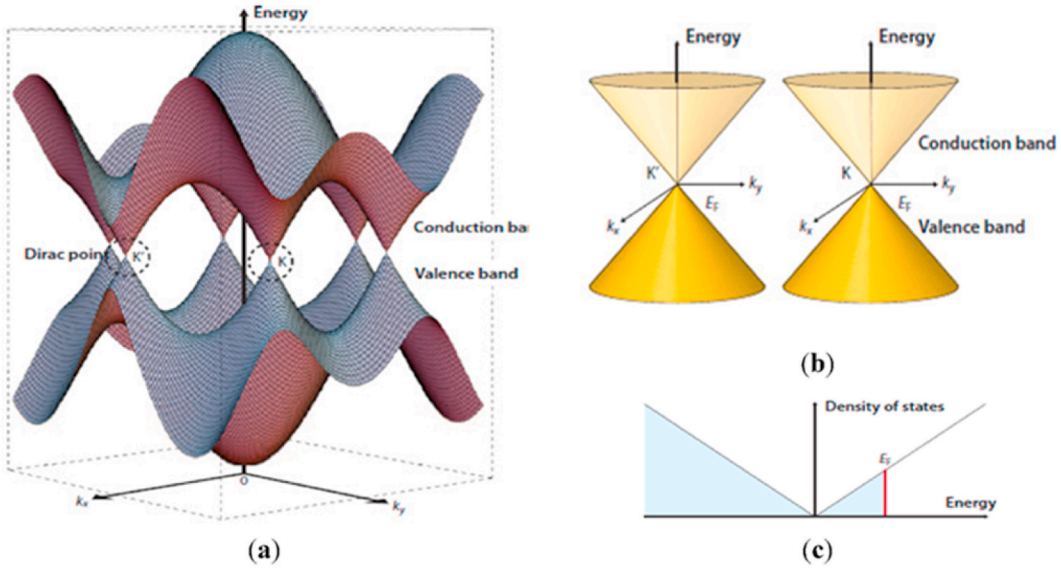

Fig. 4. (a) Schematic illustration of the energy bands near the Fermi level in graphene. The horizontal plane in the first Brillouin zone of graphene. The conduction and valence band meets at the K and K′ points in the Dirac cone. (b) The conic energy bands near the K and K′ points. (c) The density of states with the fermi energy near the Fermi level. Figure remodified from Ref. [91].

$$\delta_1 = \frac{a_1}{2}(1, 1.732) \quad \delta_2 = \frac{a_1}{2}(1, -1.732) \quad \delta_3 = -a_1(1, 0.00) \tag{4}$$

while in Eq. (5), the six closest neighbors are situated at:

$$\delta_1 = \pm a_1, \delta_2 = \pm a_2, \delta_3 = \pm (a_2 - a_1) \tag{5}$$

2.2.1. *The quantum Hall effect of graphene material*

Edwin Hall hypothesized that the magnetic field caused a transverse voltage in the wire when he reported the classical Hall-effect in the late 19th century. An electron gas with a strong magnetic field splits into Landau levels because of the magnetic field. The orbital for each level is described in Eq. (6) [92]:

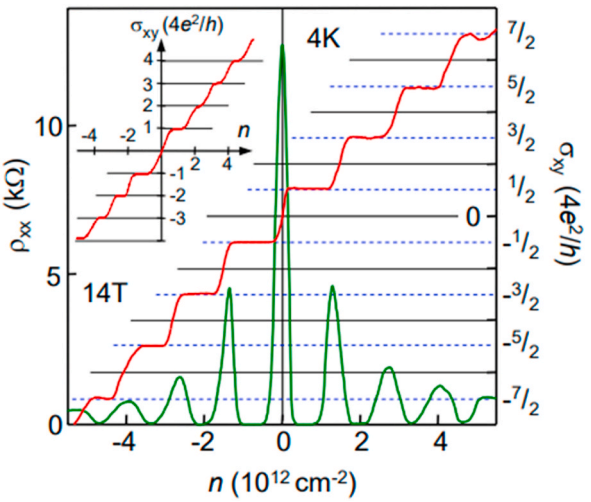

Fig. 5. The QHE for massless fermions in monolayer graphene. Hall Conductivity σ_{xy} and longitudinal resistivity ρ_{xx} of graphene as a function of their concentration at $B = 14\ T$ *and* $T = 4\ .K\ \sigma_{xy} = (2e/\sqrt{h})\ V^{\frac{1}{2}}$ is determined from the measured dependencies of $\rho_{xy}\ (V_g)$ and $\rho_{xx}\ (V_g)$ as $\sigma_{xy} = \rho_{xy}/(\rho_{xy}^2 + \rho_{xx}^2)$. The nature of $1/\rho_{xy}$ is similar but shows a discontinuity at $V_g \approx 0$, which was avoided by plotting σ_{xy}. The quantization sequence in the two-layer graphene's inset displays the σ_{xy} at integer j, where it is normal. Figure remodified from Ref. [102].

$$D = \sqrt{2\pi eB/\hbar c}\left(\frac{L}{2\pi}\right) = \left(\frac{eBL^2}{hc}\right)^{1/2} \tag{6}$$

Graphene's highly unique charge carriers exhibit massless relativistic behaviour and are one of the material's most fascinating features, i.e., the Dirac fermions as displayed in Fig. 5. When confined to magnetic fields, Dirac fermions act in a manner that is significantly aberrant in the energy spectra of the Landau levels compared to electrons, as demonstrated by the anomalous integer quantum Hall effect [93]. The Landau energy levels of graphene can be written as:

$$E_j = \pm (j) V_F (2e\hbar|j|B)^{1/2} \tag{7}$$

Therefore, Eq. (7) provides the clearest proof for the non-interacting Dirac fermion model [92]. Therefore, $j = 0, \pm 1, \pm 2,$ The Fermi velocity is represented by V_F, e is the elementary charge, where $\hbar$ the reduced Planck's constant is and can be expressed as $\hbar = \frac{h}{2\pi}$ and B represents the magnetic field.

However, the chiral quasiparticles show that graphite possesses a Berry phase 2 that is dominated by a parabolic dispersion and a double-degenerate zero-energy. The Landau level contains two distinct orbital states ($K - K'$ points) with the same energy, i.e., both the electrons and holes share the same level [93,94]. This reveals the anomalous integer QHE where Eq. (8) describes the Hall conductivity [93]:

$$\sigma_{xy} = \pm \frac{(4j+2)e^2}{h} \tag{8}$$

The electronic structure of graphene, however, exhibits an anomalous quantization that is replaced by a non-empty, half-integer Berry's phase. The quantum Hall effect in a single layer of graphene is sharply different from the standard QHE for both holes and electrons. This sets graphene apart from other traditional 2D carbon-based electronic materials with a definite carrier mass [95,96]. The anomalous quantum hall-effect was first reported by Novoselov et al. [96] which is illustrated in Fig. 5a. This is calculated at B = T and T = 4 K [96]. As a result, the charge Hall conductance is precisely quantized as described in Eq. (9), when the Fermi level is in the energy gap [93]:

$$\sigma_{xy} = \frac{2e^2}{h} \tag{9}$$

Furthermore, Qiao et al. [97] reveal that Rashba spin-orbit coupling, and exchange fields can cause graphene to develop a visible gap. Furthermore, a gap as large as 5.5 meV appeared at the Dirac points, resulting in a topological effect using first-principles calculations. This further validates the anomalous QHE in graphene [98]. Thus, a Dirac cone is created by plotting the energy of the topological electrons against momentum indicating graphene has a very high thermal conductivity [99,100]. Moreover, Cynse et al. [101] discovered a fourfold splitting in the Coulomb interaction for quantum hall. It is possible to produce a Hamiltonian that only contains graphene and correctly depicts the impurity by using first-principles calculations and a genetic algorithm technique. The physics of graphene exhibits a pronounced breaking of the structure for lower Landau levels, high magnetic fields, and fast-moving electrons, and this disorder exponentially increases with the magnetic field.

2.3. The optical properties of pure graphene material

Electronic transitions are fundamental for the optical properties of solids in general. They are inextricably linked to their electronic structures and are crucial to their application. As a result, optical anisotropy has been observed in graphene superlattices, with the level of anisotropy being determined by the thickness of the graphene layer and not the composition [103] Furthermore, the empirical results have demonstrated that the optical and energy loss spectra of graphene indicate a redshift of absorption bands and the $\pi + \sigma$ electron plasmon, as well as the removal of mass plasmons, as contrasted to graphite [104,105]. The optical properties, absorption coefficient, reflectivity, complex refractive index, dielectric function, etc. Have been investigated in several studies. The dielectric function specifies the features of electromagnetic waves as they flow through a medium by describing the linear response of the medium to electromagnetic radiation [106–109]. The complex dielectric function is expressed in Eq. (10) below:

$$\varepsilon(\omega) = \varepsilon_1(\omega) + i\varepsilon_2(\omega) \tag{10}$$

Hence, ω is the photon frequency, $\varepsilon_1(\omega)$ and $\varepsilon_2\ (\omega)$ are the real and imaginary parts of the complex dielectric function in Eq. (10), respectively [110]. In more detail, Fermi's golden rule is as follows in Eq. (11) because of the direct inter-band transition [111]:

$$\varepsilon_2(\omega) = \frac{2e^2\pi}{\Omega\varepsilon_0} \sum_{k,c,v} \left|\left(\Psi_k^c \middle| u \bullet r \middle| \Psi_k^v\right)\right|^2 \delta\left(E_k^c - E_k^v - E\right) \tag{11}$$

ω = The electromagnetic radiation's frequency, Ω = volume of the cell, ε_0 = permittivity of free space, c = conduction band, v = valence band, u = vectors characterized by the polarization of the incident electric field, and r = vector location.

The real and imaginary parts $\varepsilon_2(w)$ of a dielectric function $\varepsilon_1(\omega)$ can be compared using the Kramers-Kroing relation in Eq. (12) [111].

$$\varepsilon_1(\omega) = \frac{1}{\pi} P \int_{-\infty}^{\infty} \varepsilon_2 \frac{\omega'}{\omega' - \omega} d\omega' \quad (12)$$

P represents the integral's primary value.

The amount of energy lost by the wave when it passes through a solid is indicated by the light absorption coefficient [111]. Moreover, despite its high absorption coefficient, one-atom-thick graphene absorbs only 0.023 of visible light and has a reflectance of less than 0.001 of infrared light, according to several experimental findings [112–114]. This is due to the linear dispersion of the electron, which causes it to behave like a massless material, which is amazing for a monolayer material [115–117]. However, this is rather poor for applications in photodetection [118,119]. Hence, the absorbed white light is determined by the atomic structure and not the properties of the material [120]. The amount of white light absorbed increases linearly [121,122]. In addition, graphene is a promising candidate for sensing broadband in the terahertz and infrared ranges, but this results in its short exciton lifetime, which is harmful to exciton splitting and high photoresponsivity [123–125]. Moreover, graphene's absorption spectrum is empty in the ultraviolet region, ranging from (900–300) $\times$ 10^{-9} m, with a maximum absorption peak about 270 nm [126]. In summary, several studies established that graphene has a Drude-like intra-band conductivity based on $\Omega = 0$, followed by an area of reduced conductivity at higher energies before a sudden rise to a steady comprehensive framework value of $\sigma_0 = \pi e^2/2h$ indicating that graphene exhibits semi-metallic behaviour [125,127,128]. The transitions between the fully filled valence band and the unfilled conduction band are known as inter-band transitions, and this accounts for its optical sensitivity [129–132]. However, an extensive study is required on the optical properties of graphene employing the density functional calculations to tailor it for applications in optoelectronics.

2.4. Modification of the electronic and optical properties of graphene by chemical doping

This is employed to modify the intrinsic behaviour of graphene to achieve optimized performance by doping a controlled percentage of foreign atoms in its symmetry [133,134]. The formation energy, bond length and band gap of the different doped graphene structures reported in literature are displayed in Table 1. Meanwhile there are two methods reported for the chemical doping of graphene generally: (1) The adsorption of specified materials such as gases, chemicals, metals among others into the graphene surface. (2) Foreign atoms are substituted into graphene, replacing the C atom. Therefore, the substitution of heteroatoms for the carbon atoms in graphene induces structural and electronic changes, contributing to the modifications of the system's thermal, carrier mobility, fermi level, electronic and optical properties [135–137]. This can result in either a nucleophile (electron donor), an n type or an electrophile (electron acceptor), a p type semiconductor. Nitrogen (n-type) and boron (p-type) are the most studied dopant atom because of their similar atomic radii to carbon, with nitrogen having an extra electron and boron being electron-deficient [138–140]. However, nitrogen has attracted more interest than boron due to its ease of substitution into graphene [141,142]. Moreover, the Graphitic-N (sp^2 hybridization), pyridinic (sp^2 hybridization), and pyrrolic N (sp^3 hybridization) are the three most common N bonding configurations [143]. Studies shows that the pyridinic-N bonding configuration is relatively stable in the presence of mono-vacancy while pyrrolic bonding energetically favours divacancy defect [144–146]. The graphitic configuration favours an n-type while both pyrrolic and pyridinic favours a p-type doping [147]. Fig. 6(a) and (b) reveals the structural and electronic band

Table 1
The calculated parameters for pure and different doped graphene systems.

System (%)	Band Gap (eV)	Bond length (Å)	Formation energy (eV)	References
Graphene	0.00	1.42	NA	[155–157]
Beryllium doped Graphene (12.50)	1.44	1.56	25.56	[158,159]
Beryllium doped Graphene (12.50)	1.44 0.89	1.46	2.96	[160,161]
Beryllium doped Graphene (25.00)	1.42	1.55	5.19 25.56	[110,162]
Boron doped Graphene (12.00)	0.32	1.42	1.42	[163,164]
Boron doped Graphene	0.30	1.47	3.46	[165–167]
Boron doped Graphene	0.32	1.49	−27.30	[168]
Sulphur doped Graphene	0.57	1.62	8.33	[162,169]
Silicon doped Graphene (6.25)	0.70	1.65	−0.87	[170]
Silicon doped Graphene	2.00	1.91	NA	[171]
Nitrogen doped graphene	1.30	1.39	0.32	[172,173]
Nitrogen doped Graphene	0.21	1.39	−6.63	[157,174]
Phosphorous doped Graphene (3.13)	0.32	1.77	−6.42	[175–177]
Aluminium doped Graphene	0.40	1.73	9.86	[157,169]
Iron doped Graphene	1.70	1.67	7.24	[174,178,179]
Nitrogen-Aluminium doped Graphene	0.47	1.69	13.5 13.4	[157]
Beryllium–Nitrogen doped Graphene (25.00)	1.54	1.75	13.54	[158,180]
Beryllium-Sulphur doped Graphene	0.58	(Be) 1.53–1.54 (S) 1.36–1.38	2.45	[162]
Beryllium-Sulphur doped Graphene	0.37	NA	4.85	[181]

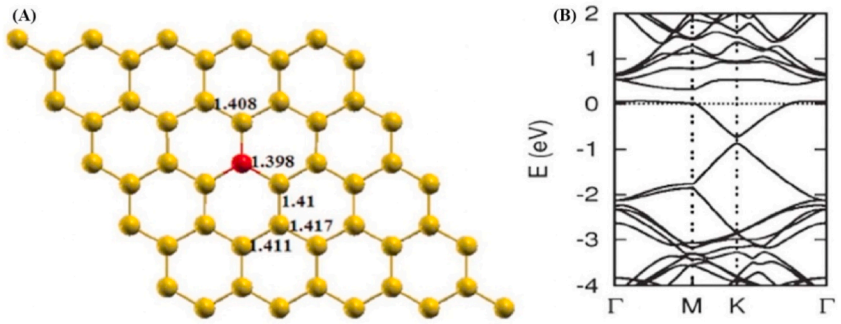

Fig. 6. The (a) optimized geometry and (b) the electronic band structure of Nitrogen-doped graphene. The Nitrogen atom is symbolized by the red ball and the bond lengths indicated in the rings are measured in Å. Figure remodified from Ref. [107]. (For interpretation of the references to colour in this figure legend, the reader is referred to the Web version of this article.)

change of a N/G graphene. Moreover, Rafique et al. [148] observed that nitrogen doping preserves linear energy dispersion around graphene's Dirac cone using the ab initio method. The studies on N-doped graphene have focused on the influence of the total percentage of N-doping in graphene, while few studies have investigated the positions of the N-dopant atom and the impact of the different C–N bonding configurations. However, B-doped graphene, as revealed by Beheshti and his colleagues, results in an electron-deficient structure [148].

Likewise, Be-doped graphene are reported in literature. However, despite its physical and electronic potentials as indicated by density functional approach, it suffers from very high formation energy which has limited its viability for synthesis compared to the N- and B-doped graphene [110]. Nonetheless, atomic elements with larger atomic radii than carbon such as silicon, sulphur, germanium are being substituted into graphene lattice to modify its intrinsic properties [149–151]. Moreover, Marinopoulos et al. [152] reports that the graphite's absorption spectra for the light parallel to the c axis and the increasing of interlayer spacing resulted in the stacking of the graphene layers unit cell with less intense mutual interaction [152]. The absorption spectra of the graphene sheet structures are displayed in Fig. 7b and (c). At the same time, Nath et al. [153] compared the reflectivity of pure graphene to that of B/N doped graphene and observed a redshift of the main peak at higher doping concentration (See Fig. 8) [154]. However, despite the potentials of employing *ab* initio studies to chemically dope graphene reported in literature several discrepancies exist in their results (see Tables 1–5) which may be as a result of the choice of the exchange correlations functionals, and basis set as well as wrong input parameters. Meanwhile, in the next section, a brief discussion of the different generations of exchange correlation functionals

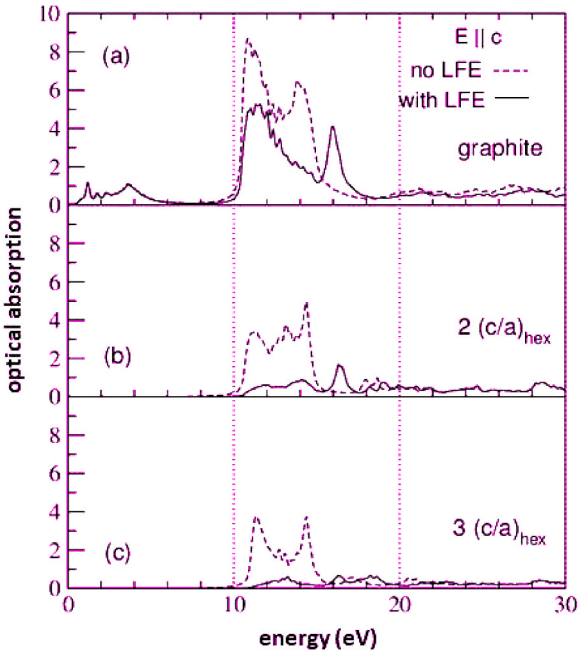

Fig. 7. (a) Graphite and (b) graphene sheet geometries with $2(c/a)_{hex}$ and (c) $3(c/a)_{hex}$ for $E \perp_C$ optical absorption spectrum. Figure remodified from Ref. [152].

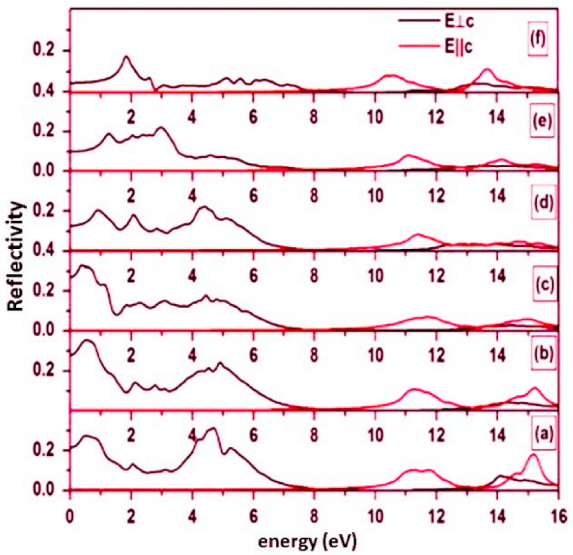

Fig. 8. The reflectivity for pristine graphene (a) as compared with graphene dual doped at different percentages of BN in increasing order of concentrations of boron at different percentages (b), 12.75% (c) 18.75% (d) and 37.5% (e) and 75% respectively for perpendicular and parallel polarization. Figure remodified from Ref. [154].

employed in density functional theory is presented. We have also surveyed machine learning, which was recently proposed as a way of improving density functional theory models by employing a large amount of training data from first principles calculations to accurately predict and tailor the properties of graphene for optoelectronics.

3. Overview of DFT models for the optoelectronic properties of graphene

3.1. Density functional models employed for predicting properties of graphene

It is one of the most popular computational approaches applied in condensed matter physics and quantum chemistry and is based on the concept that electron density can be employed as a basic variable to solve the electronic structure problem of materials as well as the total electronic energy [214–219]. It relies on the Hohenberg-Kohn's theorem and gives completely quantum solutions to solving the Schrodinger equation, by mapping the many body systems of interacting electrons into a simplified single-particle problem [220–222]. The Born-Oppenheimer approximation is used to represent the degenerate N-ground system's state energy as illustrated in Eqn. (13), which is a special functional of the electron density [223]:

$$E[\rho(r)] = F[\rho(r)] + J[\rho(r)] + Q_{ee}[\rho(r)] \tag{13}$$

where the overall functional $F[\rho(r)]$ is given by the sum of the kinetic energy functional $T[\rho(r)]$ and the nuclear-electron interaction energy functional represented by $V_{en}[\rho\,(r)]$ and the quantum electron-electron energy represented by $Q_{ee}[\rho(r)]$. Furthermore, the first attempts at density functionals were made in the early twentieth century by Thomas and Fermi theory, which predicted mutually independent movements of the electrons and a local density approximation characterizing the kinetic energy associated with the motion [224–227]. Moreover, this functional failed miserably in regions with large spatial changes in electron density [228]. However, about four decades later, Kohn and Sham demonstrated in their paper that the problem of electron kinetic energy using a basis set can be accurately approximated by a single slater determinant to represent an imaginary system of non-interacting electrons (columbic interaction ignored), with the same ground state density as the exact correlation functional [223,229,230].

The literature has reported over 300 functionals over the last three and a half decades, and with the current trend, it is expected to double in the next ten years [215,231]. These are the semi-empirical and non-empirical functionals, which envelope parameters fitted from data and free parameters deduced by fitting standard specifications, respectively [223,232,233]. A few examples of semi-empirical functionals include B3LYP, ωB97X-2, B 97, while non-empirical functionals include PBE, TPSS, SCAN, etc. However, for a detailed presentation, see Refs. [223,234–238]. Regardless, the five distinct classifications of the XC functionals are displayed in Fig. 9. This is a progressive illustration known as Jacob's ladder, which demonstrates that each rung corresponds to functionals that elicit a certain kind of approximation with the chemical accuracy increasing by moving up the ladder and is more advanced [239–242]. However, the top rung has a higher computational cost [243,244]. Moreover, the precision of the energies and electron densities increases with each step until the turn of the century [244–246]. However, the energies have continued to advance while the accuracy of the electron density is declining [247]. This could be because conventional fitting ignores characteristics with high density dependencies. However, this is debatable [247].

Table 2
A summary of the applications and gaps of doped graphene systems in literature.

Focus of Study	Comments/Inference	Prospects	Gaps	Reference
DFT study of CO adsorption in Boron-doped and Nitrogen-doped graphene (B/NG)	1. The stabilities of Nitrogen and Boron showed an anisotropy behaviour and response to CO adsorption 2. B/NG doping is a more effective gas detector due to its high sensitivity. 3. B/NG improves adsorption energy.	Chemical Sensor of toxic gases	1. Limited theoretical studies in relation to doping sites on the composition of co-doping of B/NG 2. Reduced Charge transfer	[182–184]
DFT study of the adsorption of boron doped graphene (B/G)	1. It turns to a less electronegative network. 2. It is an efficient storage material for Li-Ion batteries 3. Induces P-type conductivity	Li-ion Batteries	1. Broken symmetry which implies structural deformities 2. Different doped graphene structures are not stable.	[185,186]
First principles calculations of calculations of calcium decorated boron doped graphene	1. Boron doping limits clustering problem by increasing metal adsorption strength on graphene compared to Transition metal coated graphene	Hydrogen Storage	1. Individual Calcium atoms are not stable on graphene. 2. Weaker bond observed in the B-doped graphene system	[187]
Ab initio calculations of the electronic structure of Boron and Nitrogen doped graphene sheets	1. Graphene changed from a semi-metal to semiconductor with an increasing number of dopants. 2. The size of the band gap is determined by the lattice position of the dopant atoms.	Polymer-based electrolytic fuel cells	1. There are variations in the stability of the doped systems.	[107]
Ab initio studies of the geometry, and electronic properties of Beryllium and Boron doped graphene	1. The percentage and the position of the dopants is important in modifying the band structure of graphene. 2. The band gap created can be used to design transistor devices. 3. Hexagonal doping was reported to be superior to rectangular doping due to its higher band gap	Electronic devices	1. Rectangular doping engineered a lower band gap. 2. At higher doping percentage the symmetry was broken and a decrease in the cohesive energy	[159]
Ab initio study of doping of Alkaline earth (Be, Mg, Ca, and Sr) metals on graphene	1. A full electron transfer of $a + 1.6e^{-}$ was observed for Be/G. 2. Spin polarized electronic structures and ionic bonding observed in (Mg, Ca, Sr) indicating magnetic properties. 3. They are energetically stable revealing its viability as a doping motif	Magnetic Semiconductors	1. Be/G does not exhibit any magnetic properties. 2. Inconsistency in the charged transfer compared to existing results	[188]

Table 3
A summary of the different doping types, applications, and gaps of doped graphene systems in literature.

System	Doping Type	Applications	Gaps in Literature	References
1. Dissociation of H_2S on Fe-doped graphene 2. Adsorption of NO on Fe-doped graphene.	N-type Semiconductor	Sensors Low dimensional materials	1. In adsorption with H_2S the impact of Fe with S is weak at certain distances 2. Instability in the interactions between the adsorbent and adsorbate which results in the desorption process due to the positive electric fields	[178,189]
Aluminium doped graphene	N-type Semiconductor	Sensors	1. Less efficient than Beryllium doped graphene in terms of electronic engineering 2. High formation energy associated with its unusual reactivity. 3. Low rate of absorption in the Visible light range.	[157,190]
Sulphur doped graphene	N-type Semiconductor	Electronic devices	1. Decrease in the work function and band gap at higher doping concentration. 2. It has poor magnetic moment 3. Large formation energy which affects the ease of substitution into graphene when compared into nitrogen dopants.	[191,192]
Platinum doped graphene	N-type Semiconductor	Electronics, Optoelectronics, and sensors.	1. Structural deformities in graphene 2. Rare atomic elements 3. Limited theoretical and experimental studies	[193]

Table 4
A summary of the different doping types, applications, and gaps of doped graphene systems in literature.

System	Doping Type	Applications	Gaps in Literature	References
Pure graphene	NA	Electronics, Photonics, Optoelectronic devices, etc.	1. Its intrinsic electrical conductivity and very high resistivity limit its rate of absorption. 2. Zero-band gap	[194–196]
Beryllium doped graphene. Be-decorated Fullerenes.	P-type Semiconductor	Nano-electronics and Optoelectronic devices Hydrogen Storage Transistors	1. Very large formation energy, and poor stability. 2. Reduced charge transfer 3. Decrease in the volume of H_2 adsorbed due to the dissociation of H_2 molecule. 4. No record of its experimental synthesis in literature based on our knowledge.	[158,159,197]
Boron doped graphene	P-type Semiconductor	Electronic devices. Optoelectronic devices Li-ion batteries Circuits, Memory devices	1. Less effective in engineering the band structure of graphene 2. In the long wavelength limit for parallel polarization, the static dielectric constant depends on the impurity concentration. 3. No absorption at high doping percentage. 4. Poor catalytic activity in Non-aqueous Li-ion batteries	[159,163,165, 168,198–200]
Hydrogen adsorption on Nitrogen-doped graphene.	N-type Semiconductor (Graphitic) P-type semiconductor (pyrrolic and pyridinic)	Optoelectronics devices	1. The role of each of the C–N bonding configuration remain elusive 2. There was a rapid decrease in the absorption coefficient in the visible light range.	[13,46,172, 201–203]
Silicon doped graphene	P-type Semiconductor	Semiconducting devices	1. Lower effective masses for the carriers of siliphene compared to traditional semiconductors such as Si and GaAs 2. Very wide band gap may not be suitable for field effect transistors 3. Clustering of silicon atom in graphene at higher doping concentration.	[169,171, 204–206]

Table 5
A summary of the different doping types, applications, and gaps of doped graphene systems in literature.

System	Doping Type	Applications	Gaps in Literature	References
1. B-/N doped graphene	N-type Semiconductor	Fast Computer Processors, Circuits	1. Weak contributions of the π electrons resulting in decrease in the electronic conductivity 2. Large redshift in the absorption coefficient towards the visible light spectrum 3. Torsional deformation at the main peak	[107,172,202, 207–210]
Be-/N doped graphene	P-type semiconductor	Nano-electronics and optoelectronic devices	Beryllium still has large formation energy although much reduced despite co-doping with Nitrogen and decrease in stability despite indicating the possibilities of being synthesized at high doping concentrations.	[110]
Be-/S doped graphene	N-type semiconductor	Electronic and Optoelectronic devices	1. The system's stability falls with an increase in the dopants concentration which is evidenced by the defects formed in the system. 2. Reduced optical peak intensities at higher doping concentration.	[211,212]
N–Al doped graphene	N-type Semiconductor	Electronic devices	Large formation energy impedes its stability. Poor optical absorption	[213]

Additionally, the orbital shell describes the characteristics of solids. As a result, Herring postulated that an orbital's base during World War II is an orthogonalized plane wave, which is a linear combination of core and plane waves (OPW) [248,249]. Convergence restrictions were present in this model, although this was overcome by using secular determinants in the OPW and pseudopotentials developed by Philip and Kleinman [250,251]. The pseudopotentials describe the interaction between the nuclei and the core electrons and enable the modelling of crystals such as graphene with any atomic element on the periodic table [252–255]. Examples of widely used pseudopotentials embedded in simulation software for calculating and modelling graphene with any atomic element are the projected augmented plane waves and ultrasoft pseudopotentials [256–258].

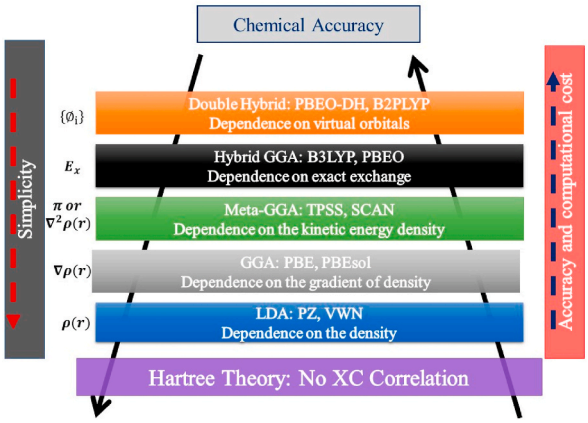

Fig. 9. The Jacob's Pardew ladder rung describing the hierarchy of the XC functionals. Figure remodified from Ref. [317,318].

Moreover, the first implementations of DFs employed LDA functionals [259,260]. However, this functional is plagued with controversies due to systematic errors and the overestimation of the interaction energies. The limitation was circumvented by GGA approximations, which consider spatial variation and not only the spin densities [261,262]. However, this failed to accurately define the localized states; it underestimates the band structure and phonon properties of crystals, even in graphene. This has resulted in the development of more advanced XC functionals, such as Meta-GGAs and hybrid functionals, which incorporate the reliance on K.E. densities and Hartree Fock, respectively, to reach chemical accuracy heaven [248,263,264]. This is displayed in Table 6, highlighting their distinguishing features. In summary, DFT is widely recognized for calculating the electronic structure of graphene due to its well-proven theories, which have been extensively validated, and an increasing volume of papers in the literature has greatly contributed to its acceptance in the scientific community [265–267]. Furthermore, the different simulation codes and platforms employed for DFT calculations are displayed in Table 7. However, density functional calculations may not accurately reflect the electronic properties of large and complex systems with strong electronic correlation or non-local effects, which is where ML-DFT functionals are handy [218,220,261]. Therefore, an overview of this newbie in computational material science is presented in the following sub-section.

3.2. *Machine learning models for predicting the properties of graphene*

Machine learning (ML), a form of computer pattern recognition that automatically improves with experience, has had a substantial impact on several fields of science during the last decade [319–322]. Moreover, in the late 20th century, Doren and co-workers noted that ML had evolved into a technique for the design of atomistic potentials by leveraging it to approximate unknown factors [323]. However, despite the challenging task of distinguishing between machine learning, a branch of artificial intelligence, and *ab initio* DFT-based calculation without some measure of arbitrariness [324,325].

The convergence of these two major fields has resulted in a new direction of deep learning first-principles calculations in computational material science and chemistry for developing systems affecting our daily lives, such as flexible electronic devices, voice recognition, and self-driving cars, among other things [324]. As a result, a variety of ML-potentials, including neural network potentials (NNPs) [326–329], Gaussian approximate potentials (GAP) [330,331], moment tensor potentials (MTP) [332,333], and kernel ridge regression (KRR) [334,335], have been reported in the literature for this purpose [336–339] A brief description of a few of the potentials used in machine learning DFT and their applications, is given in Table 8. A review of all the ML potentials is beyond the scope of this study. The potentials generate a force field or potential energy surface, which is the atomic localization of potential energy and atomic forces [340]. Furthermore, the Born-Oppenheimer approximation defines the potential energy surface (PES) [341,342]. Therefore, the training data, such as their corresponding energies, forces, and stress, can be employed to execute the Molecular dynamics simulations in determining the electronic structure with precision comparable to the ab initio approach without incurring a large computing burden [343,344]. The earliest potential, the neural network, is confined to low-dimensional systems, while the second variant is known as the high-dimensional neural network [343,345]. Here, the maximum atomic energy contributions induced by the energy vary depending on the local environment, which is characterized by atom-centered symmetry function descriptors [343, 346]. This ensures that the requirement for the linear, rotational, and permutation invariance for many body systems of any configurations is met [347–349]. The descriptors are the central element of the ML model, which has to do with an iterative process known as the numerical encoding of the input cases or materials [350].

Moreover, the prediction scheme should possess a numerical encoding to be considered quantitative [351,352]. However, a sufficient understanding of the problems and goals is essential in the right selection of the numerical encoding which considers the materials properties related to the intended property [352]. The descriptor may need to incorporate important information regarding the atomic level elements that may govern these behaviours since the accuracy required of the predictions depends on the relevant characteristics or a specified property of a 2D material, such as the optical properties of graphene [353]. Moreover, the common

Table 6
A summary of the different XC functionals employed in density functional calculations.

Functional	Description	Strengths	Weakness	Uncertainties	References
Local Density Approximation (LDA)	It makes an approximation of the XC energy, which depends on the electron density at defined points	It gives a solid representation of the chemical bond and electronic properties of graphene. Moreso, it is more efficient than the self-consistent field HF	The calculated band gap is underestimated and has poor accuracy.	The calculated results of the LDA are generally considered to be less accurate than the GGA or hybrid functionals	[268–272]
Generalized Gradient Approximation (GGA)	It relies on the local electron density gradient and the electron density	It corrects the underestimation of the calculated band gap with LDA	The calculated band gap is overestimated	They are seen as being more accurate than LDA. However, they are less reliable than the hybrid functionals	[273–276]
Hybrid Functionals	It combines the Hartree-Fock (HF) exchange integral and the exchange functional	In terms of the band gap and electronic structure of graphene, it outperforms both the LDA and GGA XC functionals	It's application in large systems is constrained by the exact exchange's expensive cost, which scales with the number of electrons	Predictions may have fewer uncertainties. However, they are more computationally expensive	[277–281]
Meta-GGA functionals	It employs the electron density, its gradient, and the K.E. density to distinguish between single orbital and orbital overlap regions	It accurately describes the electronic structure and normalizes LDA/GGA's under and overestimation of the calculated band gap	It is computationally more expensive than LDA and GGA	It has considerably larger uncertainties compared to both the LDA and GGA potentials. These are evident in the total energies, geometries, and electronic structure	[282–284]
Double hybrid Functionals	It contains a virtual K–S orbitals, in which non-local Fock exchange substitutes a portion of the semi local DFT exchange, as well as non-local effect	Better precision for molecular structures and binding energies It provides a more accurate account of the effects of long-range electron correlation caused by London dispersion forces	It is computationally more expensive than LDA and GGA Some of them have intrinsic deficiencies, such as the large basis set superposition error and missing London dispersion effects	It is laborious to determine its uncertainties because the accuracy relies on the exact functionals and system under study Undefined DF or atomic or atomic basis set combination can introduce systematic error into the system	[285,286]

Table 7
A summary of the DF's simulation codes based on their basis types.

Name	Software	License	References
Plane-waves basis sets	CASTEP	Commercial	[10–13]
	VASP	Commercial	[14–16]
	ABINIT	General Public License	[17–19]
	BigDFT	General Public License	[297,298]
Linearized augmented plane wave	WIEN2K	Commercial	[299–301]
	FLEUR	Massachusetts Institute of Technology	[302–304]
Atom centered basis set	SIESTA	General Public License	[305–307]
	ORCA	free	[308,309]
	Gaussian	Commercial	[310–312]
	Q-Chem	Commercial	[313,314]
Real-space grids	GPAW	General Public License	[315,316]

Table 8
Summary of description and applications of ML potentials.

Machine Learning Potentials	Descriptions	Applications	References
Neural Network	The neural networks are used widely in ML potentials to calculate energy and forces from atomic locations. The conventional neural networks are characterized using feed forward neural networks which can be enhanced physically to offer extrapolation capabilities outside the scope of the training data. However, it can only be employed in low dimensional systems	To predict the energetics of lithium intercalation into graphite with accuracy comparable to DFT models To enhance the rate of convergence and prediction accuracy for the inverse optical design of inverse optical design of graphene-based metamaterials	[370,372, 373]
Gaussian approximate potentials (GAP)	The total energy disintegrates into local atomic contributions which are determined using the gaussian process regression from *ab initio* data	It creates the graphene interatomic potential To predict finite temperature phonon spectra and the thermal expansion of graphene	[218,344, 374,375]
Moment Tensor potentials	It is an active learning approach that is analogous to GAP, and has descriptors based on tensor operations that essentially approximate any PES. It induces less energy and force test errors at greater precision and speed of calculation	It is trained to modeled atomic interactions To calculate thermal and mechanical properties	[369,376]

descriptor is the electronic property obtained without complicated calculations, while more accurate descriptors that include the valence band in the d-band core are computationally expensive. This implies striking a balance between the cost and prediction accuracy [354,355]. Today, the third and fourth variant descriptors were able to describe long-range interactions beyond the local chemical environments but relies on the local charges [343].

However, the predictions of the ML potentials are subject to uncertainties which are challenging to verify due to the approximate models of the real bonding physics of the system. These can either be numerical, structural, and parametric [356–359]. The factors that the numerical uncertainty considers are the size of the computational domain, and the set-up time for the input. The structural and parametric uncertainties that relate to the accuracy of the ML potentials are more burdensome [359,360]. The Bayesian approaches, the gaussian process regression offer a logical route for measuring the prediction's level uncertainty [361,362]. The Bootstrapping is an alternative, simple and flexible approach to access the uncertainties [363]. There are other approaches, but they come at a substantial additional expense. Moreover, the uncertainty can be utilized to gradually and constantly enhance prediction models which may be achieved by optimizing the costs between exploration and exploitation [364]. The uncertainty and the strength of some of these potentials are revealed in Table 9.

The ML algorithm can be grouped into supervised modelling, unsupervised modelling [365], semi-supervised modelling [366], and reinforcement modelling. The supervised learning contains both the input and the output data, i.e., label data. Unsupervised modelling is used on unlabeled data with no inherent ground truth. In addition, the se mi-supervised models have a larger input than output as they combine the strengths of supervised and unsupervised models [367,368], and the reinforcement models do not require previous knowledge and instead acquire knowledge and experience via interaction with the environment.

It is important to note that the role of model selection is to determine the best approach and parameters for a particular task [364]. Thus, the label of the input data sets, and the known physical image of descriptors and properties of interest heavily influence the selection of the most suitable approach, which is the heart of the selection process [354]. Therefore, for a comprehensive description of ML and its applications in DFT, consult refs, [218,369–371]. However, despite the exciting prospects of ML-DFT, we observed that it has not yet been widely applied to graphene in the literature, which may be a result of insufficient data sets which is required for obtaining accurate results and the complexity of the electronic structure of graphene, etc. Moreover, the existing knowledge gap in the literature, which will provide meaningful insights into the future trends and directions in study of graphene for applications in optoelectronics, are presented in the following sub-section.

Table 9
The strength, weakness, and uncertainties of ML potentials.

Name	Strength	Weakness	Uncertainties	References
Neural Network	Their non-linear functional is flexible which enables accurate and faster electronic structure calculations	1. Identifying its hyperparameters and developing training regimens that prevent overfitting can be difficult 2. Interpretability and explainability is lacking for practically accurate results for large time data	The uncertainty in the construction of the potential energy surface of graphene relies on the efficiency of the training set essential for improved transferability required of NN potential	[322,324, 377]
Gaussian Approximation Potential	It is faster than first principles approach and is independent of the size of the training set.	1. For huge data, the inference stage of GAP requires matrix inversion which increases the computing cost 2. Overfitting of the models which has resulted in unphysical behaviours 3. It fails to capture the interlayer interactions; it is not applicable to multilayer graphene structures	The transferability of GAP has a high degree of uncertainty to accurately predict outside the training set. Moreover, the specific implementation and the training set relies on the accuracy of GAP	[378,379]
Moment Tensor Potentials	It is computationally cheaper and save more time than DFT calculations.	The learning algorithm is built through a time-consuming trial and error cycles in which the trained potential efficiency is manually evaluated	This is currently being investigated and has not been completely established. However, its accuracy might be affected by the size of the configuration domain and the input data.	[380,381]

3.3. Knowledge gaps of graphene research

Despite the expanding scope of density functional theory and the emerging ML-DFT approach in providing an enormous understanding of the electronic structure at absolute temperature and optical excitations of graphene, some grey areas remain unresolved.

1. Band gap calculation: The band gap calculation of graphene structures is a controversial topic in the literature, with different exchange-correlation functionals employed in ab initio studies predicting different values due to imbalances in the delocalization, static correlation error, and the wrong selection of parameters, making the choice of XC functionals system dependent. Moreover, the lack of training data for ML models has restricted their applications in predicting the electronic properties of graphene [323].
2 Van der Waals (vdW) interactions: The inability of the XC functionals employed in the ab initio studies to describe long-range electron correlations for the properties of graphene Thus, the lack of dispersion forces is one of the most significant problems in first principles calculations [382]. Moreover, training of the non-local ML potential is system-specific, and to accurately describe the non-local functional with different parameters, a large amount of training data is required [383].
3 Vibration and Temperature Effects: The effects of the vibrations from DFT calculations are not defined for both the band structure and spectroscopy level in graphene. This limits the role of polaronic effects, including the effect of temperature, which is important for optoelectronic applications that are frequently temperature dependent.
4 Modelling of graphene-based heterostructures: There are limitations in the accurate modelling of graphene-based heterostructures, such as the graphene-hBN layer and graphene silicon heterostructures. This is due to the complexity of their systems, which involve the interaction of different parameters. This has restricted the modelling of the interactions and the properties of these heterostructures, resulting in discrepancies in the calculations of their electronic and optical properties. Moreover, ML potentials require a large time series of data to accurately predict these properties.

3.4. Future trends of graphene research

Graphene's electronic properties have received most of the interest in research to this point, whereas few models have been developed on its thermal conductivities from different illustrations of phonons and even from density functional theory, molecular dynamics simulations, and ML training data to accurately determine its phonon transport. This will improve the imagination and provide comprehensive information on graphene's phonon scattering [384]. Moreover, by exploring its thermal conductivity, it can help solve the heat dissipation problem in electronic devices and aid in the design and commercialization of high-performance future optoelectronic and thermodynamic devices, e.g., heat engines, with optimized performance and stability.

Recently, graphene/hBN heterostructures have been considered the foundation for next-generation optoelectronics due to their high electron mobilities and tunable band structure. Currently, graphene-based heterostructures are being tested in optical communication satellites, superfast electronics, and photodetectors [171]. However, accurate and transferable DFT and ML models to determine the strong anisotropic tensor in the overall optical response of graphene heterostructures are required to facilitate their implementation in real-world optical systems [385,386].

Graphene has been reported to display inherent superconducting and nonconducting behaviour by creating a superlattice of two graphene layers rotated at a magic angle of 1.1°. Therefore, employing traditional DFT and ML-DFT to accurately predict the unconventional superconducting and insulating nature of large and complex graphene are essential in the near future for the design and fabrication of nano-superconducting quantum optical devices and nano-superconducting transistors [387].

Moreso, graphene is regarded as the thinnest and strongest 2D material, which highlights its prospects for application in ultrathin and ultralight aviation composite materials. Interestingly, it also has the potential to reduce the weight of the aircraft by 1%, saving almost $1 billion in fuel usage. Moreover, graphene-based coatings with distinct electronic properties might use electricity to generate thermal energy and transport it to the external surface, or they could improve conductivity and electromagnetic shielding to guard against lightning strikes. Therefore, optimization of the DFT and ML-DFT frameworks in future studies to modify graphene's structural and electronic properties is critical for the design and large-scale manufacturing of these graphene-based devices [388,389].

4. Conclusions

This review presents a detailed theoretical foundation, models employed in density functional theory, and recent research efforts in computational material science with the aid of machine learning to accurately predict the properties of graphene. The electronic and optical properties of the chemically doped graphene systems using the DFT approach were extensively discussed, with special emphasis on their prospects, doping type, and reported gaps in the literature. Moreover, these gaps can be associated with the choice of the exchange correlation functionals, basis sets, and wrong inputs of parameters, which affect the accuracy of its predictions. Despite this, traditional DFT models are at the heart of the electronic structure calculation of graphene, and the results are validated experimentally. Similarly, recent advances in machine learning have demonstrated tremendous potential for speeding up and improving the accuracy of DFT predictions of long-range electron correlations of graphene properties. However, the results obtained from ML-DFT have not been validated experimentally yet. Hence, the marriage of these two approaches is projected to play a key role in addressing the knowledge gaps in the study of graphene and ensuring it fulfills its promise.

Author contribution statement

All authors listed have significantly contributed to the development and the writing of this article.

Funding statement

A. L. Olatomiwa acknowledges Malaysia International Scholarship (MIS) for funding his Master of Science (MSC) in Nanomaterial Engineering at the Institute of Nano Electronic Engineering, Universiti Malaysia Perlis, Malaysia.

Data availability statement

Data will be made available on request.

Declaration of interest's statement

The authors declare that they have no known competing financial interests or personal relationships that could have appeared to influence the work reported in this paper.

References

[1] C. Draxl, D. Nabok, K. Hannewald, Organic/inorganic hybrid materials: challenges for ab initio methodology, Acc. Chem. Res. 47 (2014) 3225–3232, https://doi.org/10.1021/ar500096q.
[2] J. Schmidt, M.R.G. Marques, S. Botti, M.A.L. Marques, Recent advances and applications of machine learning in solid-state materials science, NPJ Comput Mater 5 (2019), https://doi.org/10.1038/s41524-019-0221-0.
[3] Y. Zheng, Y. Jiao, M. Jaroniec, S.Z. Qiao, Advancing the electrochemistry of the hydrogen- Evolution reaction through combining experiment, Angew. Chem., Int. Ed. 54 (2015) 52–65, https://doi.org/10.1002/anie.201407031.
[4] M. Bahri, S.H. Gebre, M.A. Elaguech, F.T. Dajan, M.G. Sendeku, C. Tlili, D. Wang, Recent advances in chemical vapour deposition techniques for graphene-based nanoarchitectures: from synthesis to contemporary applications, Coord. Chem. Rev. 475 (2023), https://doi.org/10.1016/j.ccr.2022.214910.
[5] S.K. Tiwari, R.K. Mishra, S.K. Ha, A. Huczko, Evolution of graphene oxide and graphene: from imagination to industrialization, ChemNanoMat 4 (2018) 598–620, https://doi.org/10.1002/cnma.201800089.
[6] W. Ahmad, A.K. Tareen, K. Khan, M. Khan, Q. Khan, Z. Wang, M. Maqbool, A review of the synthesis, fabrication, and recent advances in mixed dimensional heterostructures for optoelectronic devices applications, Appl. Mater. Today 30 (2023), https://doi.org/10.1016/j.apmt.2022.101717.
[7] S.H. Mir, V.K. Yadav, J.K. Singh, J.K. Singh, Recent advances in the carrier mobility of two-dimensional materials: a theoretical perspective, ACS Omega 5 (2020) 14203–14211, https://doi.org/10.1021/acsomega.0c01676.
[8] M.R. Kumar, S. Singh, H.M. Fahmy, N.K. Jaiswal, S. Akin, A.E. Shalan, S. Lanceros-Mendez, M. Salado, Next generation 2D materials for anodes in battery applications, J. Power Sources 556 (2023), https://doi.org/10.1016/j.jpowsour.2022.232256.
[9] M. Naseri, Two-dimensional δ-Be2C with hepta-coordinated carbons: a highly stable direct-band-gap semiconductor predicted by first-principles calculations, J. Phys. Chem. C 127 (2023) 1687–1696, https://doi.org/10.1021/acs.jpcc.2c07834.
[10] Y. Wang, J. Liang, Z. Yang, L.C. Xu, L. Xue, R. Liu, X. Liu, Theoretical study of the line defect in χ3-borophene: structures, electronic properties, direct-current and alternating-current transport properties, Appl. Surf. Sci. 608 (2023), https://doi.org/10.1016/j.apsusc.2022.155033.
[11] V. Nagarajan, R. Bhuvaneswari, R. Chandiramouli, Adsorption studies of camphene and eucalyptol molecules on orthorhombic germanane nanosheet - a first-principles investigation, J. Mol. Graph. Model. 119 (2023), https://doi.org/10.1016/j.jmgm.2022.108395.
[12] A.P. Balan, A.B. Puthirath, S. Roy, G. Costin, E.F. Oliveira, M.A.S.R. Saadi, V. Sreepal, R. Friedrich, P. Serles, A. Biswas, S.A. Iyengar, N. Chakingal, S. Bhattacharyya, S.K. Saju, S.C. Pardo, L.M. Sassi, T. Filleter, A. Krasheninnikov, D.S. Galvao, R. Vajtai, R.R. Nair, P.M. Ajayan, Non-van der Waals quasi-2D materials; recent advances in synthesis, emergent properties and applications, Mater. Today 58 (2022) 164–200, https://doi.org/10.1016/j.mattod.2022.07.007.
[13] E.B. Yutomo, F.A. Noor, T. Winata, Effect of the number of nitrogen dopants on the electronic and magnetic properties of graphitic and pyridinic N-doped graphene-a density-functional study, RSC Adv. 11 (2021) 18371–18380, https://doi.org/10.1039/d1ra01095f.
[14] X. Xu, L.F.C. Pereira, Y. Wang, J. Wu, K. Zhang, X. Zhao, S. Bae, C. Tinh Bui, R. Xie, J.T.L. Thong, B.H. Hong, K.P. Loh, D. Donadio, B. Li, B. Özyilmaz, Length-dependent thermal conductivity in suspended single-layer graphene, Nat. Commun. 5 (2014), https://doi.org/10.1038/ncomms4689.
[15] S. Jindal, R. Anand, N. Sharma, N. Yadav, D. Mudgal, R. Mishra, V. Mishra, Sustainable approach for developing graphene-based materials from natural resources and biowastes for electronic applications, ACS Appl. Electron. Mater. 4 (2022) 2146–2174, https://doi.org/10.1021/acsaelm.2c00097.
[16] X. Xu, L.F.C. Pereira, Y. Wang, J. Wu, K. Zhang, X. Zhao, S. Bae, C. Tinh Bui, R. Xie, J.T.L. Thong, B.H. Hong, K.P. Loh, D. Donadio, B. Li, B. Özyilmaz, Length-dependent thermal conductivity in suspended single-layer graphene, Nat. Commun. 5 (2014), https://doi.org/10.1038/ncomms4689.
[17] T. de S.A. Cassiano, L.E. de Sousa, L.A. Ribeiro Junior, G.M.e. Silva, P.H. de Oliveira Neto, Charge transport in cove-type graphene nanoribbons: the role of quasiparticles, Synth. Met. 287 (2022), https://doi.org/10.1016/j.synthmet.2022.117056.
[18] R. Siburian, S. Paiman, F. Hutagalung, A.M.M. Ali, L. Simatupang, R. Goei, M.M. Rusop, Facile method to synthesize of magnesium-graphene nano sheets for candidate of primary battery electrode, Colloids Interface Sci. Commun. 48 (2022), https://doi.org/10.1016/j.colcom.2022.100612.
[19] S. Banerjee, Anderson localizaion for semi-dirac semi-weyl semi-metal. http://arxiv.org/abs/1508.05145, 2015.
[20] É. Lantagne-Hurtubise, X.X. Zhang, M. Franz, Dispersive Landau levels and valley currents in strained graphene nanoribbons, Phys. Rev. B 101 (2020), https://doi.org/10.1103/PhysRevB.101.085423.
[21] H.P. Veeravenkata, A. Jain, Density functional theory driven phononic thermal conductivity prediction of biphenylene: a comparison with graphene, Carbon 183 (2021) 893–898, https://doi.org/10.1016/j.carbon.2021.07.078.
[22] M. Milićević, G. Montambaux, T. Ozawa, O. Jamadi, B. Real, I. Sagnes, A. Lemaître, L. le Gratiet, A. Harouri, J. Bloch, A. Amo, Type-III and tilted Dirac cones emerging from flat bands in photonic orbital graphene, Phys. Rev. X 9 (2019), https://doi.org/10.1103/PhysRevX.9.031010.
[23] A.H. Khadem, T.U. Hasan, A.N.M.M. Rahman, S.A. Smriti, S. Alimuzzaman, Fabrication, properties, and performance of graphene-based textile fabrics for supercapacitor applications: a review, J. Energy Storage 56 (2022), https://doi.org/10.1016/j.est.2022.105988.
[24] M. Andelkovic, K.Y. Rakhimov, A. Chaves, G.R. Berdiyorov, M.v. Milošević, Wave-packet propagation in a graphene geometric diode, Phys. E Low Dimens. Syst. Nanostruct. 147 (2023), https://doi.org/10.1016/j.physe.2022.115607.
[25] J.H. Gosling, S.v. Morozov, E.E. Vdovin, M.T. Greenaway, Y.N. Khanin, Z. Kudrynskyi, A. Patanè, L. Eaves, L. Turyanska, T.M. Fromhold, O. Makarovsky, Graphene FETs with high and low mobilities have universal temperature-dependent properties, Nanotechnology 34 (2023), https://doi.org/10.1088/1361-6528/aca981.

[26] C. Zheng, X. Zhou, H. Cao, G. Wang, Z. Liu, Synthesis of porous graphene/activated carbon composite with high packing density and large specific surface area for supercapacitor electrode material, J. Power Sources 258 (2014) 290–296, https://doi.org/10.1016/j.jpowsour.2014.01.056.
[27] A.G. Klechikov, G. Mercier, P. Merino, S. Blanco, C. Merino, A.v. Talyzin, Hydrogen storage in bulk graphene-related materials, Microporous Mesoporous Mater. 210 (2015) 46–51, https://doi.org/10.1016/j.micromeso.2015.02.017.
[28] M. Zaheer, H. Naeem Abbasi, Fabrication and characterization of graphene coated nickel electrodes with internally stacked double layer supercapacitors, Ain Shams Eng. J. 13 (2022), https://doi.org/10.1016/j.asej.2022.101795.
[29] S. Nauriyal, T. Choudhary, H. Mehtani, V. Gupta, J. Singh, A game changer nano-fiber: review on recent trends of graphene, Mater. Today Proc. 63 (2022) 127–130, https://doi.org/10.1016/j.matpr.2022.02.402.
[30] Y. Meng, B. Li, L. Li, J. Zhang, Buckling behavior of few-layer graphene on soft substrate, Coatings 12 (2022), https://doi.org/10.3390/coatings12121983.
[31] B. Luo, L. Wu, D. Li, Z. Zhang, X. Yu, G. Li, H. Song, Novel atomic-scale graphene metamaterials with broadband electromagnetic wave absorption and ultra-high elastic modulus, Carbon 196 (2022) 146–153, https://doi.org/10.1016/j.carbon.2022.04.065.
[32] Y. Che, X. Cao, L. Du, H. Li, J. Yao, Highly photosensitive CsPbBr3 NCs-graphene phototransistor with memory function, Opt Commun. 532 (2023), https://doi.org/10.1016/j.optcom.2022.129252.
[33] P. Mahesh, D. Panigrahy, C. Nayak, A comprehensive study of tunable properties of broadband terahertz absorber based on graphene-embedded random photonic crystals, Phys. B Condens. Matter 650 (2023), https://doi.org/10.1016/j.physb.2022.414581.
[34] M.A. Iqbal, N. Anwar, M. Malik, M. Al-Bahrani, Md.R. Islam, J.R. Choi, P.V. Pham, X. Liu, Nanostructures/graphene/silicon junction-based high-performance photodetection systems: progress, challenges, and future trends, Adv. Mater. Interface (2023), 2202208, https://doi.org/10.1002/admi.202202208.
[35] S. Joseph, J. Mohan, S. Lakshmy, S. Thomas, B. Chakraborty, S. Thomas, N. Kalarikkal, A review of the synthesis, properties, and applications of 2D transition metal dichalcogenides and their heterostructures, Mater. Chem. Phys. 297 (2023), https://doi.org/10.1016/j.matchemphys.2023.127332.
[36] A. Sharma, G. Gupta, Recent development and prospects for metal Selenide-based gas sensors, Mater. Sci. Eng., B 290 (2023), 116333, https://doi.org/10.1016/j.mseb.2023.116333.
[37] Z. Liu, J. Liu, P. Yin, Y. Ge, O.A. Al-Hartomy, A. Al-Ghamdi, S. Wageh, Y. Tang, H. Zhang, 2D Xenes: optical and optoelectronic properties and applications in photonic devices, Adv. Funct. Mater. 32 (2022), https://doi.org/10.1002/adfm.202206507.
[38] F. Xia, H. Wang, D. Xiao, M. Dubey, A. Ramasubramaniam, Two-Dimensional Material Nanophotonics, n.d.
[39] X. Zhou, Q. Deng, W. Yu, K. Liu, Z. Liu, The rise of graphene photonic crystal fibers, Adv. Funct. Mater. 32 (2022), https://doi.org/10.1002/adfm.202202282.
[40] J.E. Lee, G. Ahn, J. Shim, Y.S. Lee, S. Ryu, Optical separation of mechanical strain from charge doping in graphene, Nat. Commun. 3 (2012), https://doi.org/10.1038/ncomms2022.
[41] Z. Peng, X. Chen, Y. Fan, D.J. Srolovitz, D. Lei, Strain engineering of 2D semiconductors and graphene: from strain fields to band-structure tuning and photonic applications, Light Sci. Appl. 9 (2020), https://doi.org/10.1038/s41377-020-00421-5.
[42] R. Lv, M. Terrones, Towards new graphene materials: doped graphene sheets and nanoribbons, Mater. Lett. 78 (2012) 209–218, https://doi.org/10.1016/j.matlet.2012.04.033.
[43] X. Wang, G. Sun, P. Routh, D.H. Kim, W. Huang, P. Chen, Heteroatom-doped graphene materials: syntheses, properties and applications, Chem. Soc. Rev. 43 (2014) 7067–7098, https://doi.org/10.1039/c4cs00141a.
[44] S.J. Lee, J. Theerthagiri, P. Nithyadharseni, P. Arunachalam, D. Balaji, A. Madan Kumar, J. Madhavan, V. Mittal, M.Y. Choi, Heteroatom-doped graphene-based materials for sustainable energy applications: a review, Renew. Sustain. Energy Rev. 143 (2021), https://doi.org/10.1016/j.rser.2021.110849.
[45] Y. Zheng, Y. Jiao, M. Jaroniec, Y. Jin, S.Z. Qiao, Nanostructured metal-free electrochemical catalysts for highly efficient oxygen reduction, Small 8 (2012) 3550–3566, https://doi.org/10.1002/smll.201200861.
[46] G. Deokar, J. Jin, U. Schwingenschlögl, P.M.F.J. Costa, Chemical vapor deposition-grown nitrogen-doped graphene's synthesis, characterization and applications, NPJ 2D Mater Appl 6 (2022), https://doi.org/10.1038/s41699-022-00287-8.
[47] X. Ma, G. Ning, C. Qi, C. Xu, J. Gao, Phosphorus and nitrogen dual-doped few-layered porous graphene: a high-performance anode material for lithium-ion batteries, ACS Appl. Mater. Interfaces 6 (2014) 14415–14422, https://doi.org/10.1021/am503692g.
[48] W. Xu, T.S. Lim, H.K. Seo, S.Y. Min, H. Cho, M.H. Park, Y.H. Kim, T.W. Lee, N-doped graphene field-effect transistors with enhanced electron mobility and air-stability, Small 10 (2014) 1999–2005, https://doi.org/10.1002/smll.201303768.
[49] V. Stanev, K. Choudhary, A.G. Kusne, J. Paglione, I. Takeuchi, Artificial intelligence for search and discovery of quantum materials, Commun. Mater. 2 (2021), https://doi.org/10.1038/s43246-021-00209-z.
[50] A. Rozmysłowska-Wojciechowska, T. Wojciechowski, W. Ziemkowska, L. Chlubny, A. Olszyna, A.M. Jastrzębska, Surface interactions between 2D Ti 3 C 2/Ti 2 C MXenes and lysozyme, Appl. Surf. Sci. 473 (2019) 409–418, https://doi.org/10.1016/j.apsusc.2018.12.081.
[51] E.P. Randviir, D.A.C. Brownson, C.E. Banks, A decade of graphene research: production, applications and outlook, Mater. Today 17 (2014) 426–432, https://doi.org/10.1016/j.mattod.2014.06.001.
[52] A.F. Madsuha, Y. Kurniawan, P.A. Permana, S. Sumaedi, The sustainability of graphene research: a novel approach in assessing the role of higher education policies in developing countries—the case of Indonesia, Sustainability (2022) 14, https://doi.org/10.3390/su14010302.
[53] A. García, M. Ferrari, S.J. Rowley-Neale, C.E. Banks, Recent advances in 2D hexagonal boron nitride (2D-hBN) applied as the basis of electrochemical sensing platforms, n.d.. https://doi.org/10.1007/s00216-020-03068-8/Published.
[54] A.K. Geim, Graphene prehistory, Phys. Scripta (2012), https://doi.org/10.1088/0031-8949/2012/T146/014003.
[55] N.G. Prikhod'ko, Z.A. Mansurov, M. Auelkhankyzy, B.T. Lesbaev, M. Nazhipkyzy, G.T. Smagulova, Flame synthesis of graphene layers at low pressure, Russ. J. Phys. Chem. B 9 (2015) 743–747, https://doi.org/10.1134/S1990793115050115.
[56] D.J. Hsu, Y.W. Chi, K.P. Huang, C.C. Hu, Electrochemical activation of vertically grown graphene nanowalls synthesized by plasma-enhanced chemical vapor deposition for high-voltage supercapacitors, Electrochim. Acta 300 (2019) 324–332, https://doi.org/10.1016/j.electacta.2019.01.134.
[57] H~chstlamellarer Kohlenstoff aus Graphit-oxyhydroxyd, n.d.
[58] H. Boehm, R. Setton, E. Stumpp (93; Germany); C. Chatillon (1989-93; France); J. B. Clark (1985-91; South Africa); J.-P. Coutures (1985-87; France); J. Drowart (1985-87; Belgium), W.-L. Ng, 1994.
[59] D.R. Dreyer, S. Park, C.W. Bielawski, R.S. Ruoff, The chemistry of graphene oxide, Chem. Soc. Rev. 39 (2010) 228–240, https://doi.org/10.1039/b917103g.
[60] P.R. Wallace, P.R.W. Ace, The Band Theory of Graphite, 1947.
[61] S. Ullah, P.A. Denis, R.B. Capaz, F. Sato, Theoretical characterization of hexagonal 2D Be3N2 monolayers, New J. Chem. 43 (2019) 2933–2941, https://doi.org/10.1039/c8nj05600e.
[62] S.S. Varghese, S. Swaminathan, K.K. Singh, V. Mittal, Energetic stabilities, structural and electronic properties of monolayer graphene doped with boron and nitrogen atoms, Electronics 5 (2016), https://doi.org/10.3390/electronics5040091.
[63] A.K. Geim, K.S. Novoselov, The rise of graphene, 2009. www.nature.com/naturematerials.
[64] A.D. Pingale, A. Owhal, A.S. Katarkar, S.U. Belgamwar, J.S. Rathore, Facile synthesis of graphene by ultrasonic-assisted electrochemical exfoliation of graphite, in: Mater Today Proc, Elsevier Ltd, 2021, pp. 467–472, https://doi.org/10.1016/j.matpr.2020.10.045.
[65] M.S. Dresselhaus, P.T. Araujo, Perspectives on the 2010 nobel prize in physics for graphene, ACS Nano 4 (2010) 6297–6302, https://doi.org/10.1021/nn1029789.
[66] B. Comeau, M.A. Jones, Labs 7-9 growing and observing micro and nanostructures, n.d, https://ocw.mit.edu/help/faq-fair-use.
[67] R.S. Koen Houtsma, J. de La Rie, M. Stö, Atomically precise graphene nanoribbons: interplay of structural and electronic properties, Chem. Soc. Rev. 50 (2021) 6541, https://doi.org/10.1039/d0cs01541e.
[68] J.v. Anguita, M. Ahmad, S. Haq, J. Allam, S.R.P. Silva, Nanotechnology: ultra-broadband light trapping using nanotextured decoupled graphene multilayers, Sci. Adv. 2 (2016), https://doi.org/10.1126/sciadv.1501238.
[69] A.H. Castro Neto, F. Guinea, N.M.R. Peres, K.S. Novoselov, A.K. Geim, The electronic properties of graphene, Rev. Mod. Phys. 81 (2009) 109–162, https://doi.org/10.1103/RevModPhys.81.109.

[70] K.S. Novoselov, S.v. Morozov, T.M.G. Mohinddin, L.A. Ponomarenko, D.C. Elias, R. Yang, I.I. Barbolina, P. Blake, T.J. Booth, D. Jiang, J. Giesbers, E.W. Hill, A. K. Geim, Electronic properties of graphene, in: Phys Status Solidi B Basic Res, 2007, pp. 4106–4111, https://doi.org/10.1002/pssb.200776208.

[71] H. Agarwal, B. Terrés, L. Orsini, A. Montanaro, V. Sorianello, M. Pantouvaki, K. Watanabe, T. Taniguchi, M. Romagnoli, F.H.L. Koppens, 2D-3D integration of hexagonal boron nitride and a high-κ dielectric for ultrafast graphene-based electro-absorption modulators, n.d. https://doi.org/10.1038/s41467-021-20926-w.

[72] M.A. Nazir, T. Mahmood, N. Akhtar, K. Hussain, W.S. Khan, M.A. Waqar, F.E. Aleem, A. Saeed, M. Fareed-Un-Nabi Saqi, J. Raza, Effect of high pressure on structural, electrical, and optical properties of graphene-like zinc oxide (g-ZnO) structure, Mater. Sci. Semicond. Process. 142 (2022), 106465, https://doi.org/10.1016/J.MSSP.2022.106465.

[73] D.M. Chen, P.M. Shenai, Y. Zhao, Tight binding description on the band gap opening of pyrene-dispersed graphene, Phys. Chem. Chem. Phys. 13 (2011) 1515–1520, https://doi.org/10.1039/c0cp00909a.

[74] F. Akbar, · M Kolahdouz, S. Larimian, · B Radfar, · H H Radamson, Graphene synthesis, characterization and its applications in nanophotonics, nanoelectronics, and nanosensing, n.d. https://doi.org/10.1007/s10854-015-2725-9.

[75] S.K. Tiwari, S. Sahoo, N. Wang, A. Huczko, Graphene research and their outputs: status and prospect, J. Sci.: Adv. Mater. Dev. 5 (2020) 10–29, https://doi.org/10.1016/J.JSAMD.2020.01.006.

[76] Y. Gao, D. Xu, T. Cui, D. Li, Stability of hydrogen-terminated graphene edges, Phys. Chem. Chem. Phys. 23 (2021) 13261–13266, https://doi.org/10.1039/d1cp01384j.

[77] M.O. Goerbig, J.-N. Fuchs, G. Montambaux, F. Piechon, Tilted Anisotropic Dirac Cones in Quinoid-type Graphene and Alpha-(bedt-TTF)_2I_3, 2008, https://doi.org/10.1103/PhysRevB.78.045415.

[78] G. Yang, L. Li, M.C. Ng, Structure of Graphene and its Disorders: a Review, 2018, https://doi.org/10.1080/14686996.2018.1494493.

[79] J. Wang, F. Ma, M. Sun, Graphene, Hexagonal Boron Nitride, and Their Heterostructures: Properties and Applications, 2017, https://doi.org/10.1039/c7ra00260b.

[80] Y. Obeng, P. Srinivasan, Graphene: is it the future for semiconductors? An overview of the material, devices, and applications, Electrochem. Soc. Interface 20 (2011) 47–52, https://doi.org/10.1149/2.F05111if.

[81] X.S. Dai, T. Shen, Y. Feng, H.C. Liu, Structure, electronic and optical properties of Al, Si, P doped penta-graphene: a first-principles study, Phys. B Condens. Matter 574 (2019), 411660, https://doi.org/10.1016/J.PHYSB.2019.411660.

[82] C.-Y. Lin, R.-B. Chen, Y.-H. Ho, M.-F. Lin, Electronic and Optical Properties of Graphite-Related Systems, 2017. http://arxiv.org/abs/1705.02879.

[83] M.F. Craciun, S. Russo, M. Yamamoto, S. Tarucha, Tuneable electronic properties in graphene, Nano Today 6 (2011) 42–60, https://doi.org/10.1016/J.NANTOD.2010.12.001.

[84] M. Zhang, D. Lei, X. Yin, L. Chen, Q. Li, Y. Wang, T. Wang, Magnetite/graphene composites: microwave irradiation synthesis and enhanced cycling and rate performances for lithium ion batteries, J. Mater. Chem. 20 (2010) 5538–5543, https://doi.org/10.1039/c0jm00638f.

[85] D.R. Cooper, B. D'Anjou, N. Ghattamaneni, B. Harack, M. Hilke, A. Horth, N. Majlis, M. Massicotte, L. Vandsburger, E. Whiteway, V. Yu, Experimental review of graphene, ISRN Condens. Matter Phys. 2012 (2012) 1–56, https://doi.org/10.5402/2012/501686.

[86] Y. Tang, Z. Liu, X. Dai, Z. Yang, W. Chen, D. Ma, Z. Lu, Theoretical study on the Si-doped graphene as an efficient metal-free catalyst for CO oxidation, Appl. Surf. Sci. 308 (2014) 402–407, https://doi.org/10.1016/J.APSUSC.2014.04.189.

[87] S.K. Tiwari, S. Sahoo, N. Wang, A. Huczko, Graphene research and their outputs: status and prospect, J. Sci.: Adv. Mater Devices 5 (2020) 10–29, https://doi.org/10.1016/J.JSAMD.2020.01.006.

[88] K. Hosen, B.K. Moghal, A.S.M.J. Islam, M.S. Islam, Vacancy induced electron-phonon interaction of single layer graphene, in: 2018 21st International Conference of Computer and Information Technology, ICCIT 2018, Institute of Electrical and Electronics Engineers Inc., 2019, https://doi.org/10.1109/ICCITECHN.2018.8631940.

[89] A. Feher, E. Syrkin, S. Feodosyev, I. Gospodarev, K. Kravchenko, 5 quasi-particle spectra on substrate and embedded graphene monolayers, n.d, www.intechopen.com.

[90] A.H. Castro Neto, F. Guinea, N.M.R. Peres, K.S. Novoselov, A.K. Geim, The electronic properties of graphene, Rev. Mod. Phys. 81 (2009) 109–162, https://doi.org/10.1103/RevModPhys.81.109.

[91] T. Ando, The electronic properties of graphene and carbon nanotubes, NPG Asia Mater. 1 (2009) 17–21, 10.1038/10.1038/asiamat.2009.1.

[92] X. Du, I. Skachko, F. Duerr, A. Luican, E.Y. Andrei, Fractional quantum Hall effect and insulating phase of Dirac electrons in graphene, Nature 462 (2009), https://doi.org/10.1038/nature08522.

[93] V. Singh, D. Joung, L. Zhai, S. Das, S.I. Khondaker, S. Seal, Graphene based materials: past, present and future, Prog. Mater. Sci. 56 (2011) 1178–1271, https://doi.org/10.1016/J.PMATSCI.2011.03.003.

[94] E. McCann, V.I. Fal'ko, Landau-level degeneracy and quantum hall effect in a graphite bilayer, Phys. Rev. Lett. 96 (2006) 1–4, https://doi.org/10.1103/PhysRevLett.96.086805.

[95] Y. Zhang, Y.W. Tan, H.L. Stormer, P. Kim, Experimental observation of the quantum Hall effect and Berry's phase in graphene, Nature 438 (2005) 201–204, https://doi.org/10.1038/nature04235.

[96] K.S. Novoselov, A.K. Geim, S.v. Morozov, D. Jiang, M.I. Katsnelson, I.v. Grigorieva, S.v. Dubonos, A.A. Firsov, Two-dimensional gas of massless Dirac fermions in graphene, Nature 438 (2005) 197–200, https://doi.org/10.1038/nature04233.

[97] Z. Qiao, S.A. Yang, W. Feng, W.K. Tse, J. Ding, Y. Yao, J. Wang, Q. Niu, Quantum anomalous Hall effect in graphene from Rashba and exchange effects, Phys. Rev. B Condens. Matter 82 (2010), https://doi.org/10.1103/PhysRevB.82.161414.

[98] Z. Qiao, S.A. Yang, W. Feng, W.K. Tse, J. Ding, Y. Yao, J. Wang, Q. Niu, Quantum anomalous Hall effect in graphene from Rashba and exchange effects, Phys. Rev. B Condens. Matter 82 (2010) 3–6, https://doi.org/10.1103/PhysRevB.82.161414.

[99] E. Apresyan, Some Aspects of Quantum Hall Effect 2, 2019.

[100] K. Hatsuda, H. Mine, T. Nakamura, J. Li, R. Wu, S. Katsumoto, J. Haruyama, Evidence for a quantum spin hall phase in graphene decorated with Bi2Te3 nanoparticles, Sci. Adv. 4 (2018) 1–7, https://doi.org/10.1126/sciadv.aau6915.

[101] T.P. Cysne, J.H. Garcia, A.R. Rocha, T.G. Rappoport, Quantum Hall effect in graphene with interface-induced spin-orbit coupling, Phys. Rev. B 97 (2018), https://doi.org/10.1103/PhysRevB.97.085413.

[102] K.S. Novoselov, A.K. Geim, S.v. Morozov, D. Jiang, M.I. Katsnelson, I.v. Grigorieva, S.v. Dubonos, A.A. Firsov, Two-dimensional gas of massless Dirac fermions in graphene, Nature 438 (2005) 197–200, https://doi.org/10.1038/nature04233.

[103] M. Jin, N. Jiao, H.X. Da, K.W. Zhang, X. Chen, L.Z. Sun, Anisotropic optical properties of graphene/graphane superlattices, Solid State Sci. 40 (2015) 71–76, https://doi.org/10.1016/J.SOLIDSTATESCIENCES.2014.12.018.

[104] P. Rani, • V K Jindal, Stability and electronic properties of isomers of B/N co-doped graphene, n.d. https://doi.org/10.1007/s13204-013-0280-3.

[105] Y. Murakami, E. Einarsson, T. Edamura, S. Maruyama, Polarization dependence of the optical absorption of single-walled carbon nanotubes, Phys. Rev. Lett. 94 (2005), https://doi.org/10.1103/PhysRevLett.94.087402.

[106] F. Ostovari, M. Hasanpoori, M. Abbasnejad, M.A. Salehi, DFT calculations of graphene monolayer in presence of Fe dopant and vacancy, Phys. B Condens. Matter 541 (2018) 6–13, https://doi.org/10.1016/J.PHYSB.2018.04.023.

[107] P. Rani, V.K. Jindal, Designing band gap of graphene by B and N dopant atoms, RSC Adv. 3 (2013) 802–812, https://doi.org/10.1039/c2ra22664b.

[108] S. Wang, L. Sun, S. Iqbal, Green financing role on renewable energy dependence and energy transition in E7 economies, Renew. Energy 200 (2022) 1561–1572, https://doi.org/10.1016/j.renene.2022.10.067.

[109] D. Wang, L. Yang, J. Cao, Torsion control of the electronic and optical properties of monolayer WS2: a first-principles study, Chem. Phys. 546 (2021), https://doi.org/10.1016/j.chemphys.2021.111181.

[110] O. Olaniyan, R.E. Maphasha, M.J. Madito, A.A. Khaleed, E. Igumbor, N. Manyala, A systematic study of the stability, electronic and optical properties of beryllium and nitrogen co-doped graphene, Carbon 129 (2018) 207–227, https://doi.org/10.1016/j.carbon.2017.12.014.

[111] Y. Zhang, J. Yun, K. Wang, X. Chen, Z. Yang, Z. Zhang, J. Yan, W. Zhao, First-principle study of graphyne-like BN sheet: electronic structure and optical properties, Comput. Mater. Sci. 136 (2017) 12–19, https://doi.org/10.1016/J.COMMATSCI.2017.04.006.

[112] A.F. Carvalho, B. Kulyk, A.J.S. Fernandes, E. Fortunato, F.M. Costa, A review on the applications of graphene in mechanical transduction, Adv. Mater. 34 (2022), https://doi.org/10.1002/adma.202101326.

[113] A. Woessner, Exploring flatland nano-optics with graphene plasmons, n.d. http://www.tdx.cat/?locale-.

[114] L. Matthes, O. Pulci, F. Bechstedt, Optical properties of two-dimensional honeycomb crystals graphene, silicene, germanene, and tinene from first principles, New J. Phys. 16 (2014), https://doi.org/10.1088/1367-2630/16/10/105007.

[115] H.K. Kelardeh, U. Saalmann, J.M. Rost, Ultrashort laser-driven dynamics of massless Dirac electrons generating valley polarization in graphene, Phys Rev Res 4 (2022), https://doi.org/10.1103/PhysRevResearch.4.L022014.

[116] S. Husain, I. Samad Wani, M. Aggarwal, M. Alam, H. Habib, Latest Fabrication Approaches for Surface Modified Carbon Materials: Carbon Nanotubes and Graphene, 2022, https://doi.org/10.1021/bk-2022-1424.ch002.

[117] T. Wang, Special exceptional point acting as Dirac point in one dimensional PT -symmetric photonic crystal, New J. Phys. 24 (2022), 113016, https://doi.org/10.1088/1367-2630/ac9a9f.

[118] M. Naghipoor, M. Zavvari, H. Rasooli Saghai, Two-color photodetection of graphene-based transistors enhanced by metallic photonic crystals, J. Comput. Electron. 21 (2022) 953–959, https://doi.org/10.1007/s10825-022-01886-w.

[119] Z. He, S. Zhang, L. Zheng, Z. Liu, G. Zhang, H. Wu, B. Wang, Z. Liu, Z. Jin, G. Wang, Si-based NIR tunneling heterojunction photodetector with interfacial engineering and 3D-graphene integration, IEEE Electron. Device Lett. 43 (2022) 1818–1821, https://doi.org/10.1109/LED.2022.3203474.

[120] X. Xiao, Y. Zhang, L. Zhou, B. Li, L. Gu, Photoluminescence and fluorescence quenching of graphene oxide: a review, Nanomaterials 12 (2022), https://doi.org/10.3390/nano12142444.

[121] A.J. Auty, N. Mansouriboroujeni, T. Nagaraja, D. Chekulaev, C.M. Sorensen, S.R. Das, N. Martsinovich, A.A.P. Chauvet, Ultrafast transient absorption spectroscopy of inkjet-printed graphene and aerosol gel graphene films: effect of oxygen and morphology on carrier relaxation dynamics, J. Phys. Chem. C 126 (2022) 7949–7955, https://doi.org/10.1021/acs.jpcc.2c01086.

[122] H. Chnafa, M. Mekkaoui, A. Jellal, A. Bahaoui, Transmission in Strained Graphene Subjected to Laser and Magnetic Fields, 2022. http://arxiv.org/abs/2206.03089.

[123] T.M. Radadiya, A Properties of Graphene Zaiko Warehouse Management Systems Application Platform View Project Tarun Radadiya A Properties of Graphene, 2015. www.eajournals.org.

[124] Z. Sun, H. Chang, Graphene and graphene-like two-dimensional materials in photodetection: mechanisms and methodology, ACS Nano 8 (2014) 4133–4156, https://doi.org/10.1021/nn500508c.

[125] S. Sett, A. Parappurath, N.K. Gill, N. Chauhan, A. Ghosh, Engineering sensitivity and spectral range of photodetection in van der Waals materials and hybrids, Nano Express 3 (2022), https://doi.org/10.1088/2632-959X/ac46b9.

[126] J. Phiri, P. Gane, T.C. Maloney, General overview of graphene: production, properties and application in polymer composites, Mater. Sci. Eng., B 215 (2017) 9–28, https://doi.org/10.1016/J.MSEB.2016.10.004.

[127] Z. Guo, J. Li, J. Weng, J. Li, S. Chen, P. Xu, W. Liu, K. Wen, Y. Qin, Multiple and tunable plasmon induced transparency with L-shape graphene strips structure at terahertz frequency, Opt Commun. 521 (2022), https://doi.org/10.1016/j.optcom.2022.128559.

[128] M. Mortezaei Nobahari, Anisotropic Kubo conductivity of electric field-induced monolayer β12-borophene, RSC Adv. 12 (2021) 648–654, https://doi.org/10.1039/d1ra07945j.

[129] J. Hwang, J.P.F. Leblanc, J.P. Carbotte, Optical self-energy in graphene due to correlations, J. Phys. Condens. Matter 24 (2012), https://doi.org/10.1088/0953-8984/24/24/245601.

[130] S. Mukherjee, T.P. Kaloni, Electronic properties of boron- and nitrogen-doped graphene: a first principles study, J. Nanoparticle Res. 14 (2012), https://doi.org/10.1007/s11051-012-1059-2.

[131] M. Taghizadeh, F. Bozorgzadeh, G.H. Bordbar, All-optical diffraction and ultrafast switching in a terahertz-driven quantized graphene system, Opt Laser. Technol. 159 (2023), 108969, https://doi.org/10.1016/j.optlastec.2022.108969.

[132] M. Fang, H. Gu, Z. Guo, J. Liu, L. Huang, S. Liu, Temperature and thickness dependent dielectric functions of MoTe2 thin films investigated by spectroscopic ellipsometry, Appl. Surf. Sci. 605 (2022), https://doi.org/10.1016/j.apsusc.2022.154813.

[133] M. Zhang, Y. Xu, H. Zhang, Z. Duan, T. Ren, Z. Wang, X. Li, L. Wang, H. Wang, Synergistic coupling of P-doped Pd4S nanoparticles with P/S-co-doped reduced graphene oxide for enhanced alkaline oxygen reduction, Chem. Eng. J. 429 (2022), https://doi.org/10.1016/j.cej.2021.132194.

[134] S. Ullah, Q. Shi, J. Zhou, X. Yang, H.Q. Ta, M. Hasan, N.M. Ahmad, L. Fu, A. Bachmatiuk, M.H. Rümmeli, Advances and trends in chemically doped graphene, Adv. Mater. Interface 7 (2020), https://doi.org/10.1002/admi.202000999.

[135] C. Kayklarll, D. Uzunsoy, E.D.Ş. Parmak, M.F. Fellah, Ö.Ç. Çaklr, Boron and nitrogen doping in graphene: an experimental and density functional theory (DFT) study, Nano Express 1 (2020), https://doi.org/10.1088/2632-959X/ab89e9.

[136] J.N. Zhang, L. Ma, M. Zhang, L.C. Ma, J.M. Zhang, First-principles study of the electronic and optical properties of nitrogen and gold co-doped graphene, Superlattice Microst. 139 (2020), 106363, https://doi.org/10.1016/J.SPMI.2019.106363.

[137] H. Wang, T. Maiyalagan, X. Wang, Review on recent progress in nitrogen-doped graphene: synthesis, characterization, and its potential applications, ACS Catal. 2 (2012) 781–794, https://doi.org/10.1021/cs200652y.

[138] A. Sahithi, K. Sumithra, Adsorption and sensing of CO and NH3on chemically modified graphene surfaces, RSC Adv. 10 (2020) 42318–42326, https://doi.org/10.1039/d0ra06760a.

[139] A. Sahithi, K. Sumithra, Adsorption and sensing of CO and NH3on chemically modified graphene surfaces, RSC Adv. 10 (2020) 42318–42326, https://doi.org/10.1039/d0ra06760a.

[140] L.K. Putri, B.J. Ng, W.J. Ong, H.W. Lee, W.S. Chang, S.P. Chai, Engineering nanoscale p-n junction: via the synergetic dual-doping of p-type boron-doped graphene hybridized with n-type oxygen-doped carbon nitride for enhanced photocatalytic hydrogen evolution, J. Mater. Chem. A Mater. 6 (2018) 3181–3194, https://doi.org/10.1039/c7ta09723a.

[141] M. Preeyanghaa, E.S. Erakulan, R. Thapa, M. Ashokkumar, B. Neppolian, Scrutinizing the role of tunable carbon vacancies in g-C3N4 nanosheets for efficient sonophotocatalytic degradation of Tetracycline in diverse water matrices: experimental study and theoretical calculation, Chem. Eng. J. 452 (2023), https://doi.org/10.1016/j.cej.2022.139437.

[142] C.N.R. Rao, K. Gopalakrishnan, A. Govindaraj, Synthesis, properties and applications of graphene doped with boron, nitrogen and other elements, Nano Today 9 (2014) 324–343, https://doi.org/10.1016/J.NANTOD.2014.04.010.

[143] M. Son, S.S. Chee, S.Y. Kim, W. Lee, Y.H. Kim, B.Y. Oh, J.Y. Hwang, B.H. Lee, M.H. Ham, High-quality nitrogen-doped graphene films synthesized from pyridine via two-step chemical vapor deposition, Carbon 159 (2020) 579–585, https://doi.org/10.1016/J.CARBON.2019.12.095.

[144] H. Wang, T. Maiyalagan, X. Wang, Review on recent progress in nitrogen-doped graphene: synthesis, characterization, and its potential applications, ACS Catal. 2 (2012) 781–794, https://doi.org/10.1021/cs200652y.

[145] N.I. Ikhsan, A. Pandikumar, Doped-Graphene Modified Electrochemical Sensors, Graphene-Based Electrochemical Sensors for Biomolecules: A Volume in Micro and Nano Technologies, 2019, pp. 67–87, https://doi.org/10.1016/B978-0-12-815394-9.00003-0.

[146] T. Granzier-Nakajima, K. Fujisawa, V. Anil, M. Terrones, Y.-T. Yeh, Controlling Nitrogen Doping in Graphene with Atomic Precision: Synthesis and Characterization, n.d. https://doi.org/10.3390/nano9030425.

[147] X. Wang, G. Sun, P. Routh, D.-H. Kim, W. Huang, P. Chen, Heteroatom-doped graphene materials: syntheses, properties and applications, Chem. Soc. Rev. 43 (2014) 7067, https://doi.org/10.1039/c4cs00141a.

[148] M. Rafique, Y. Shuai, I. Ahmed, R. Shaikh, M.A. Tunio, Tailoring electronic and optical parameters of bilayer graphene through boron and nitrogen atom co-substitution; an ab-initio study, Appl. Surf. Sci. 480 (2019) 463–471, https://doi.org/10.1016/J.APSUSC.2019.02.240.

[149] F. López-Urías, R. Lv, H. Terrones, M. Terrones, Characterization, and Applications, 2013.

[150] F. López-Urías, R. Lv, H. Terrones, M. Terrones, Characterization, and Applications, 2013.
[151] X. Wu, Y. Chen, Z. Xing, C.W.K. Lam, S.S. Pang, W. Zhang, Z. Ju, Advanced carbon-based anodes for potassium-ion batteries, Adv. Energy Mater. 9 (2019), https://doi.org/10.1002/aenm.201900343.
[152] A.G. Marinopoulos, L. Reining, A. Rubio, V. Olevano, Ab initio study of the optical absorption and wave-vector-dependent dielectric response of graphite, Phys. Rev. B Condens. Matter 69 (2004), https://doi.org/10.1103/PhysRevB.69.245419.
[153] P. Nath, S. Chowdhury, D. Sanyal, D. Jana, Ab-initio calculation of electronic and optical properties of nitrogen and boron doped graphene nanosheet, Carbon 73 (2014) 275–282, https://doi.org/10.1016/J.CARBON.2014.02.064.
[154] P. Rani, G.S. Dubey, V.K. Jindal, DFT study of optical properties of pure and doped graphene, Physica E Low Dimens Syst Nanostruct 62 (2014) 28–35, https://doi.org/10.1016/J.PHYSE.2014.04.010.
[155] H. Gao, Z. Liu, DFT Study of NO Adsorption on Pristine Graphene, 2017, https://doi.org/10.1039/c6ra27137e.
[156] Z. Khodadadi, Evaluation of H2S sensing characteristics of metals–doped graphene and metals-decorated graphene: insights from DFT study, Physica E Low Dimens. Syst. Nanostruct. 99 (2018) 261–268, https://doi.org/10.1016/J.PHYSE.2018.02.022.
[157] X. Zhou, C. Zhao, G. Wu, J. Chen, Y. Li, DFT study on the electronic structure and optical properties of N, Al, and N-Al doped graphene, Appl. Surf. Sci. 459 (2018) 354–362, https://doi.org/10.1016/J.APSUSC.2018.08.015.
[158] O. Olaniyan, R.E. Maphasha, M.J. Madito, A.A. Khaleed, E. Igumbor, N. Manyala, A systematic study of the stability, electronic and optical properties of beryllium and nitrogen co-doped graphene, Carbon 129 (2018) 207–227, https://doi.org/10.1016/J.CARBON.2017.12.014.
[159] S. Ullah, A. Hussain, W. Syed, M.A. Saqlain, I. Ahmad, O. Leenaerts, A. Karim, Band-gap tuning of graphene by Be doping and Be, B co-doping: A DFT study, n. d. www.rsc.org/advances.
[160] S. Ullah, P.A. Denis, F. Sato, Beryllium doped graphene as an efficient anode material for lithium-ion batteries with significantly huge capacity: a DFT study, Appl. Mater. Today 9 (2017) 333–340, https://doi.org/10.1016/J.APMT.2017.08.013.
[161] D. Li, Y. Ouyang, J. Li, Y. Sun, L. Chen, Hydrogen storage of beryllium adsorbed on graphene doping with boron: first-principles calculations, Solid State Commun. 152 (2012) 422–425, https://doi.org/10.1016/j.ssc.2011.11.042.
[162] O. Olaniyan, R.E. Mapasha, D.Y. Momodu, M.J. Madito, A.A. Kahleed, F.U. Ugbo, A. Bello, F. Barzegar, K. Oyedotun, N. Manyala, Exploring the stability and electronic structure of beryllium and sulphur co-doped graphene: a first principles study, RSC Adv. 6 (2016) 88392–88402, https://doi.org/10.1039/c6ra17640b.
[163] Y. Fujimoto, Formation, Energetics, and Electronic Properties of Graphene Monolayer and Bilayer Doped with Heteroatoms, 2015, https://doi.org/10.1155/2015/571490.
[164] F. López-Urías, M. Terrones, H. Terrones, Beryllium doping graphene, graphene-nanoribbons, C60-fullerene, and carbon nanotubes, Carbon 84 (2015) 317–326, https://doi.org/10.1016/j.carbon.2014.11.053.
[165] R. Sharma, S. Khan, V. Goyal, V. Sharma, K.S. Sharma, Investigation on effect of boron and nitrogen substitution on electronic structure of graphene, FlatChem 1 (2017) 20–33, https://doi.org/10.1016/J.FLATC.2016.10.001.
[166] M. Goudarzi, S.S. Parhizgar, J. Beheshtian, Electronic and optical properties of vacancy and B, N, O and F doped graphene: DFT study, Opto-Electron. Rev. 27 (2019) 130–136, https://doi.org/10.1016/j.opelre.2019.05.002.
[167] H.T. Larijani, M. Khorshidian, Theoretical insight into the role of pyridinic nitrogen on the catalytic activity of boron-doped graphene towards oxygen reduction reaction, Appl. Surf. Sci. 492 (2019) 826–842, https://doi.org/10.1016/j.apsusc.2019.05.149.
[168] H.R. Jiang, T.S. Zhao, L. Shi, P. Tan, L. An, First-principles study of nitrogen-, boron-doped graphene and Co-doped graphene as the potential catalysts in nonaqueous Li-O2 batteries, J. Phys. Chem. C 120 (2016) 6612–6618, https://doi.org/10.1021/acs.jpcc.6b00136.
[169] P.A. Denis, Band gap opening of monolayer and bilayer graphene doped with aluminium, silicon, phosphorus, and sulfur, Chem. Phys. Lett. 492 (2010) 251–257, https://doi.org/10.1016/j.cplett.2010.04.038.
[170] M. Rafique, Y. Shuai, N. Hussain, First-principles study on silicon atom doped monolayer graphene, Phys. E Low Dimens. Syst. Nanostruct. 95 (2018) 94–101, https://doi.org/10.1016/J.PHYSE.2017.09.012.
[171] M.S.S. Azadeh, A. Kokabi, M. Hosseini, M. Fardmanesh, Tunable bandgap opening in the proposed structure of silicon-doped graphene, Micro Nano Lett. 6 (2011) 582–585, https://doi.org/10.1049/mnl.2011.0195.
[172] R. Muhammad, Y. Shuai, H.P. Tan, First-principles study on hydrogen adsorption on nitrogen doped graphene, Phys. E Low Dimens. Syst. Nanostruct. 88 (2017) 115–124, https://doi.org/10.1016/J.PHYSE.2016.12.012.
[173] Y. Fujimoto, S. Saito, Formation, stabilities, and electronic properties of nitrogen defects in graphene, Phys. Rev. B Condens. Matter 84 (2011), https://doi.org/10.1103/PhysRevB.84.245446.
[174] J. Zhang, S. Li, Theoretical investigation on the Ni atom-pair supported by N-doped graphene for the oxygen reduction reaction, Comput. Theor. Chem. 1209 (2022), https://doi.org/10.1016/j.comptc.2022.113598.
[175] X.S. Dai, T. Shen, Y. Feng, H.C. Liu, Structure, electronic and optical properties of Al, Si, P doped penta-graphene: a first-principles study, Phys. B Condens. Matter 574 (2019), 411660, https://doi.org/10.1016/J.PHYSB.2019.411660.
[176] M.D. Esrafili, Electric field assisted activation of CO2 over P-doped graphene: a DFT study, J. Mol. Graph. Model. 90 (2019) 192–198, https://doi.org/10.1016/j.jmgm.2019.05.008.
[177] X.S. Dai, T. Shen, H.C. Liu, DFT study on electronic and optical properties of graphene modified by phosphorus, Mater. Res. Express 6 (2019), https://doi.org/10.1088/2053-1591/ab29bc.
[178] H.P. Zhang, X.G. Luo, H.T. Song, X.Y. Lin, X. Lu, Y. Tang, DFT study of adsorption and dissociation behavior of H2S on Fe-doped graphene, Appl. Surf. Sci. 317 (2014) 511–516, https://doi.org/10.1016/J.APSUSC.2014.08.141.
[179] D. Cortés-Arriagada, N. Villegas-Escobar, A DFT analysis of the adsorption of nitrogen oxides on Fe-doped graphene, and the electric field induced desorption, Appl. Surf. Sci. 420 (2017) 446–455, https://doi.org/10.1016/j.apsusc.2017.05.162.
[180] A. Hussain, S. Ullah, M.A. Farhan, Fine tuning the band-gap of graphene by atomic and molecular doping: a density functional theory study, RSC Adv. 6 (2016) 55990–56003, https://doi.org/10.1039/c6ra04782c.
[181] O. Olaniyan, E. Igumbor, A.A. Khaleed, A.A. Mirghni, N. Manyala, Ab-initio Study of the Optical Properties of Beryllium-Sulphur Co-doped Graphene Articles you may be Interested in, 2019, https://doi.org/10.1063/1.5060708.
[182] L.F. Velázquez-López, S.M. Pacheco-Ortin, R. Mejía-Olvera, E. Agacino-Valdés, DFT study of CO adsorption on nitrogen/boron doped-graphene for sensor applications, J. Mol. Model. 25 (2019), https://doi.org/10.1007/s00894-019-3973-z.
[183] Y.H. Zhang, Y. bin Chen, K.G. Zhou, C.H. Liu, J. Zeng, H.L. Zhang, Y. Peng, Improving gas sensing properties of graphene by introducing dopants and defects: a first-principles study, Nanotechnology 20 (2009), https://doi.org/10.1088/0957-4484/20/18/185504.
[184] A.S. Rad, S.S. Shabestari, S.A. Jafari, M.R. Zardoost, A. Mirabi, N-doped graphene as a nanostructure adsorbent for carbon monoxide: DFT calculations, Mol. Phys. 114 (2016) 1756–1762, https://doi.org/10.1080/00268976.2016.1145748.
[185] X. Wang, Z. Zeng, H. Ahn, G. Wang, First-principles study on the enhancement of lithium storage capacity in boron doped graphene, Appl. Phys. Lett. 95 (2009), https://doi.org/10.1063/1.3259650.
[186] K.Z. Milowska, M. Woinska, M. Wierzbowska, Contrasting Elastic Properties of Heavily B- and N-Doped Graphene, with Random Distributions Including Aggregates, 2013, https://doi.org/10.1021/jp403552k.
[187] E. Beheshti, A. Nojeh, P. Servati, A first-principles study of calcium-decorated, boron-doped graphene for high capacity hydrogen storage, Carbon 49 (2011) 1561–1567, https://doi.org/10.1016/j.carbon.2010.12.023.
[188] A.F. Christian Serraon, J.D. Anne Del Rosario, P.-Y. Abel Chuang, M. Nan Chong, Y. Morikawa, A.B. Abraham Padama, J.D. Ocon, Alkaline Earth Atom Doping-Induced Changes in the Electronic and Magnetic Properties of Graphene: a Density Functional Theory Study †, 2021, https://doi.org/10.1039/d0ra08115a.
[189] D. Cortés-Arriagada, N. Villegas-Escobar, A DFT analysis of the adsorption of nitrogen oxides on Fe-doped graphene, and the electric field induced desorption, Appl. Surf. Sci. 420 (2017) 446–455, https://doi.org/10.1016/J.APSUSC.2017.05.162.

[190] Z.M. Ao, J. Yang, S. Li, Q. Jiang, Enhancement of CO detection in Al doped graphene, Chem. Phys. Lett. 461 (2008) 276–279, https://doi.org/10.1016/J.CPLETT.2008.07.039.

[191] Y. Qu, J. Ding, H. Fu, H. Chen, J. Peng, Investigation on tunable electronic properties of semiconducting graphene induced by boron and sulfur doping, Appl. Surf. Sci. 542 (2021), https://doi.org/10.1016/j.apsusc.2020.148763.

[192] D. Mombrú, M. Romero, R. Faccio, Á.W. Mombrú, Electronic and optical properties of sulfur and nitrogen doped graphene quantum dots: a theoretical study, Phys. E Low Dimens. Syst. Nanostruct. 113 (2019) 130–136, https://doi.org/10.1016/j.physe.2019.05.004.

[193] S. Kumar, S. Sharma, R. Karmaker, D. Sinha, DFT study on the structural, optical and electronic properties of platinum group doped graphene, Mater. Today Commun. 26 (2021), 101755, https://doi.org/10.1016/J.MTCOMM.2020.101755.

[194] P. Rani, G.S. Dubey, V.K. Jindal, DFT study of optical properties of pure and doped graphene, Phys. E Low Dimens. Syst. Nanostruct. 62 (2014) 28–35, https://doi.org/10.1016/J.PHYSE.2014.04.010.

[195] L. Wei, G.L. Liu, D.Z. Fan, G.Y. Zhang, Density functional theory study on the electronic structure and optical properties of S absorbed graphene, Phys. B Condens. Matter 545 (2018) 99–106, https://doi.org/10.1016/J.PHYSB.2018.05.044.

[196] X. Mu, X. Wu, T. Zhang, D.B. Go, T. Luo, Thermal Transport in Graphene Oxide-From Ballistic Extreme to Amorphous Limit, 2014, https://doi.org/10.1038/srep03909.

[197] H. Lee, B. Huang, W. Duan, J. Ihm, Ab initio study of beryllium-decorated fullerenes for hydrogen storage, J. Appl. Phys. 107 (2010), https://doi.org/10.1063/1.3387750.

[198] M. Goudarzi, S.S. Parhizgar, J. Beheshtian, Electronic and optical properties of vacancy and B, N, O and F doped graphene: DFT study, Opto-Electron. Rev. 27 (2019) 130–136, https://doi.org/10.1016/J.OPELRE.2019.05.002.

[199] W.-J. Ong, S. Elumalai, M. Yoshimura, C.-Y. Su, Scalable One-Pot Synthesis of Nitrogen and Boron Co-doped Few Layered Graphene by Submerged Liquid Plasma Exfoliation, 2019, https://doi.org/10.3389/fmats.2019.00216.

[200] P. Lazar, R. Zbořil, M. Pumera, M. Otyepka, Chemical nature of boron and nitrogen dopant atoms in graphene strongly influences its electronic properties, Phys. Chem. Chem. Phys. 16 (2014) 14231–14235, https://doi.org/10.1039/c4cp01638f.

[201] X. Zhou, C. Zhao, G. Wu, J. Chen, Y. Li, DFT study on the electronic structure and optical properties of N, Al, and N-Al doped graphene, Appl. Surf. Sci. 459 (2018) 354–362, https://doi.org/10.1016/j.apsusc.2018.08.015.

[202] N.R. Abdullah, H.O. Rashid, M.T. Kareem, C.S. Tang, A. Manolescu, V. Gudmundsson, Effects of bonded and non-bonded B/N codoping of graphene on its stability, interaction energy, electronic structure, and power factor, Phys. Lett., Sect. A: Gen., Atom. Solid State Phys. 384 (2020), https://doi.org/10.1016/j.physleta.2020.126350.

[203] X. Wang, G. Sun, P. Routh, D.H. Kim, W. Huang, P. Chen, Heteroatom-doped graphene materials: syntheses, properties and applications, Chem. Soc. Rev. 43 (2014) 7067–7098, https://doi.org/10.1039/c4cs00141a.

[204] S. Reich, C. Thornsen, J. Maultzsch, Carbon Nanotubes Basic Concepts and Physical Properties, n.d.

[205] P.A. Denis, When noncovalent interactions are stronger than covalent bonds: bilayer graphene doped with second row atoms, aluminum, silicon, phosphorus and sulfur, Chem. Phys. Lett. 508 (2011) 95–101, https://doi.org/10.1016/J.CPLETT.2011.04.018.

[206] P.A. Denis, C. Pereyra Huelmo, A.S. Martins, Band gap opening in dual-doped monolayer graphene, J. Phys. Chem. C 120 (2016) 7103–7112, https://doi.org/10.1021/acs.jpcc.5b11709.

[207] R. Sharma, S. Khan, V. Goyal, V. Sharma, K.S. Sharma, Investigation on effect of boron and nitrogen substitution on electronic structure of graphene, FlatChem 1 (2017) 20–33, https://doi.org/10.1016/j.flatc.2016.10.001.

[208] T.A. Amollo, G.T. Mola, M.S.K. Kirui, V.O. Nyamori, Graphene for thermoelectric applications: prospects and challenges, Crit. Rev. Solid State Mater. Sci. 43 (2018) 133–157, https://doi.org/10.1080/10408436.2017.1300871.

[209] D. Fan, G. Liu, L. Wei, Electronic theoretical study on the influence of torsional deformation on the electronic structure and optical properties of BN-doped graphene, Mod. Phys. Lett. B 32 (2018), https://doi.org/10.1142/S0217984918501798.

[210] C. Huang, L. Han, L. Wu, R. Su, J. Chen, P. Lu, Electronic structure and optical properties of boron-sulfur symmetric codoping in 4 × 4 graphene systems, Eur. Phys. J. B 88 (2015) 147, https://doi.org/10.1140/epjb/e2015-60064-y.

[211] O. Olaniyan, E. Igumbor, A.A. Khaleed, A.A. Mirghni, N. Manyala, Ab-initio Study of the Optical Properties of Beryllium-Sulphur Co-doped Graphene Articles You may be Interested in, 2019, https://doi.org/10.1063/1.5060708.

[212] O. Olaniyan, R.E. Mapasha, D.Y. Momodu, M.J. Madito, A.A. Kahleed, F.U. Ugbo, A. Bello, F. Barzegar, K. Oyedotun, N. Manyala, Exploring the stability and electronic structure of beryllium and sulphur co-doped graphene: a first principles study, RSC Adv. 6 (2016) 88392–88402, https://doi.org/10.1039/c6ra17640b.

[213] X. Zhou, C. Zhao, G. Wu, J. Chen, Y. Li, DFT study on the electronic structure and optical properties of N, Al, and N-Al doped graphene, Appl. Surf. Sci. 459 (2018) 354–362, https://doi.org/10.1016/j.apsusc.2018.08.015.

[214] Q. Tang, Z. Zhou, Z. Chen, Innovation and discovery of graphene-like materials via density-functional theory computations, Wiley Interdiscip. Rev. Comput. Mol. Sci. 5 (2015) 360–379, https://doi.org/10.1002/wcms.1224.

[215] P. Morgante, R. Peverati, The devil in the details: a tutorial review on some undervalued aspects of density functional theory calculations, Int. J. Quant. Chem. 120 (2020), https://doi.org/10.1002/qua.26332.

[216] R.O. Jones, Density functional theory: its origins, rise to prominence, and future, Rev. Mod. Phys. 87 (2015), https://doi.org/10.1103/RevModPhys.87.897.

[217] W. Kohn, Nobel Lecture: Electronic Structure of Matter-Wave Functions and Density Functionals*, 1998.

[218] L. Fiedler, K. Shah, M. Bussmann, A. Cangi, A Deep Dive into Machine Learning Density Functional Theory for Materials Science and Chemistry, 2021. http://arxiv.org/abs/2110.00997.

[219] D. Gambino, O.I. Malyi, Z. Wang, B. Alling, A. Zunger, Density functional description of spin, lattice, and spin-lattice dynamics in antiferromagnetic and paramagnetic phases at finite temperatures, Phys. Rev. B 106 (2022), https://doi.org/10.1103/PhysRevB.106.134406.

[220] R. Pederson, B. Kalita, K. Burke, Machine Learning and Density Functional Theory, 2022, https://doi.org/10.1038/s42254-022-00470-2.

[221] Y. Lu, R. Zhao, J. Zhang, M. Liu, J. Gao, Minimal Active Space: NOSCF and NOSI in Multistate Density Functional Theory, n.d.

[222] B. Kanungo, N.D. Rufus, V. Gavini, Efficient All-Electron Time-dependent Density Functional Theory Calculations Using an Enriched Finite Element Basis, 2022. http://arxiv.org/abs/2210.14421.

[223] N. Mardirossian, M. Head-Gordon, Thirty years of density functional theory in computational chemistry: an overview and extensive assessment of 200 density functionals, Mol. Phys. 115 (2017) 2315–2372, https://doi.org/10.1080/00268976.2017.1333644.

[224] L.R. Domingo, M. Ríos-Gutiérrez, P. Pérez, Applications of the conceptual density functional theory indices to organic chemistry reactivity, Molecules 21 (2016), https://doi.org/10.3390/molecules21060748.

[225] J. Huang, Density-potential functional theory of electrochemical double layers: calibration on the Ag(111)-KPF $_6$ system and parametric analysis, J. Chem. Theor. Comput. (2023), https://doi.org/10.1021/acs.jctc.2c00799.

[226] X. Liu, Multiscale Methods to Investigate Mechanical Properties of Graphene, 2019, pp. 19–28, https://doi.org/10.1007/978-981-13-8703-6_2.

[227] Z. Ashraf, Ab-Initio Study of Electronic and Structural Properties for BaSnO3 Compound Using DFT Calculations and FP-LAPW Technique in Wein2k Software, 2021, https://doi.org/10.21203/rs.3.rs-325590/v1.

[228] P. Ziesche, S. Kurth, J.P. Perdew, Density Functionals from LDA to GGA, 1998.

[229] N. Argaman, G. Makov, Density Functional Theory-An Introduction, 1999.

[230] S.F. Sousa, P.A. Fernandes, M.J. Ramos, General performance of density functionals, J. Phys. Chem. A 111 (2007) 10439–10452, https://doi.org/10.1021/jp0734474.

[231] Z.M. Sparrow, B.G. Ernst, T.K. Quady, R.A. DiStasio, CASE21: Uniting Non-empirical and Semi-empirical Density Functional Approximation Strategies Using Constraint-Based Regularization, 2021. http://arxiv.org/abs/2109.12560.

[232] R.L.A. Haiduke, R.J. Bartlett, Non-empirical exchange-correlation parameterizations based on exact conditions from correlated orbital theory, J. Chem. Phys. 148 (2018), https://doi.org/10.1063/1.5025723.
[233] J.Y. Fan, Z.Y. Zheng, Y. Su, J.J. Zhao, Assessment of dispersion correction methods within density functional theory for energetic materials, Mol. Simulat. 43 (2017) 568–574, https://doi.org/10.1080/08927022.2017.1293258.
[234] R.O. Jones, Density functional theory: its origins, rise to prominence, and future, Rev. Mod. Phys. 87 (2015), https://doi.org/10.1103/RevModPhys.87.897.
[235] R.G. Parr, Density-functional theory [9], Chem. Eng. News 68 (1990) 45, https://doi.org/10.1007/978-3-642-86105-5.
[236] A. Gö, Density-functional Theory beyond the Hohenberg-Kohn Theorem, n.d.
[237] Density Functional Methods in Chemistry, Springer, New York, 1991, https://doi.org/10.1007/978-1-4612-3136-3.
[238] J. Grotendorst, Forschungszentrum Jülich, Computational Nanoscience: Do it Yourself! Winter School, 14 - 22 February 2006, Forschungszentrum Jülich, Germany ; lecture notes, n.d.
[239] J.M.L. Martin, G. Santra, Empirical double-hybrid density functional theory: a 'third way' in between WFT and DFT, Isr. J. Chem. 60 (2020) 787–804, https://doi.org/10.1002/ijch.201900114.
[240] C. Zhang, F. Tang, M. Chen, J. Xu, L. Zhang, D.Y. Qiu, J.P. Perdew, M.L. Klein, X. Wu, Modeling liquid water by climbing up Jacob's ladder in density functional theory facilitated by using deep neural network potentials, J. Phys. Chem. B 125 (2021) 11444–11456, https://doi.org/10.1021/acs.jpcb.1c03884.
[241] M. Jäger, L. Freitag, L. González, Using computational chemistry to design Ru photosensitizers with directional charge transfer, Coord. Chem. Rev. 304–305 (2015) 146–165, https://doi.org/10.1016/J.CCR.2015.03.019.
[242] N. Mardirossian, M. Head-Gordon, -V. ωb97X, A 10-parameter, range-separated hybrid, generalized gradient approximation density functional with nonlocal correlation, designed by a survival-of-the-fittest strategy, Phys. Chem. Chem. Phys. 16 (2014) 9904–9924, https://doi.org/10.1039/c3cp54374a.
[243] B.G. Janesko, Rung 3.5 density functionals: another step on Jacob's ladder, Int. J. Quant. Chem. 113 (2013) 83–88, https://doi.org/10.1002/qua.24256.
[244] I.Y. Zhang, X. Xu, On the top rung of jacob's ladder of density functional theory: toward resolving the dilemma of SIE and NCE, Wiley Interdiscip. Rev. Comput. Mol. Sci. 11 (2021), https://doi.org/10.1002/wcms.1490.
[245] J.P. Perdew, A. Ruzsinszky, J. Tao, V.N. Staroverov, G.E. Scuseria, G.I. Csonka, Prescription for the design and selection of density functional approximations: more constraint satisfaction with fewer fits, J. Chem. Phys. 123 (2005), https://doi.org/10.1063/1.1904565.
[246] L. Vega, J. Ruvireta, F. Viñes, F. Illas, Jacob's Ladder as Sketched by Escher: Assessing the Performance of Broadly-Used Density Functionals on Transition Metal Surface Properties, n.d.
[247] S. Hammes-Schiffer, A conundrum for density functional theory: DFT studies may sometimes get the right results for the wrong reasons, Science 355 (2017) 28–29, https://doi.org/10.1126/science.aal3442.
[248] N. Mehta, M. Casanova-Páez, L. Goerigk, Semi-empirical or non-empirical double-hybrid density functionals: which are more robust? Phys. Chem. Chem. Phys. 20 (2018) 23175–23194, https://doi.org/10.1039/c8cp03852j.
[249] J.v. Ortiz, Dyson-orbital concepts for description of electrons in molecules, J. Chem. Phys. 153 (2020), https://doi.org/10.1063/5.0016472.
[250] N.W. Ashcroft, The Fermi surface of aluminium, Philos. Mag. 8 (1963) 2055–2083, https://doi.org/10.1080/14786436308209098.
[251] P.J. Mel2, A Pseudopotential Examination of the Pressure Coefficients of Optical Transitions in Semiconductors*, 1967.
[252] M.L. Urquiza, M. Gatti, F. Sottile, Pseudopotential Bethe-Salpeter Calculations for Shallow-Core X-Ray Absorption Near-Edge Structures: Excitonic Effects in Al2O3, 2023. http://arxiv.org/abs/2301.04199.
[253] D.M. Thomas, Y. Asiri, N.D. Drummond, Point Defect Formation Energies in Graphene from Diffusion Quantum Monte Carlo and Density Functional Theory, 2021, https://doi.org/10.1103/PhysRevB.105.184114.
[254] M. Fuchs, M. Bockstedte, E. Pehlke, M. Scheffler, Pseudopotential Study of Binding Properties of Solids within Generalized Gradient Approximations: the Role of Core-Valence Exchange-Correlation, 1997.
[255] S.P. Kruchinin, R.I. Eglitis, V.P. Babak, I.G. Vyshyvana, S.P. Repetsky, Effects of electron correlation inside disordered crystals, Crystals 12 (2022), https://doi.org/10.3390/cryst12020237.
[256] J. Wangchhuk, S.R. Meher, Structural, electronic and magnetic properties of inverse spinel NiFe2O4: DFT + U investigation, Phys. Lett., Sect. A: Gen., Atom. Solid State Phys. 443 (2022), https://doi.org/10.1016/j.physleta.2022.128202.
[257] S. Jiao, Z. Zhang, K. Wu, L. Wan, H. Ma, J. Li, S. Chen, X. Qin, J. Liu, Z. Ding, J. Yang, Y. Li, W. Hu, L. Lin, C. Yang, KSSOLV 2.0: an efficient MATLAB toolbox for solving the Kohn-Sham equations with plane-wave basis set, Comput. Phys. Commun. 279 (2022), 108424, https://doi.org/10.1016/j.cpc.2022.108424.
[258] N.A.W. Holzwarth, M. Torrent, J.B. Charraud, M. Côté, Cubic spline solver for generalized density functional treatments of atoms and generation of atomic datasets for use with exchange-correlation functionals including meta-GGA, Phys. Rev. B 105 (2022), https://doi.org/10.1103/PhysRevB.105.125144.
[259] R. Churchill, L. Singh, The evolution of topic modeling, ACM Comput. Surv. 54 (2022) 1–35, https://doi.org/10.1145/3507900.
[260] I. Derkaoui, M. Achehboune, I. Boukhoubza, Z. el Adnani, A. Rezzouk, Improved first-principles electronic band structure for cubic (Pm $\bar{3}$m) and tetragonal (P4mm, P4/mmm) phases of BaTiO3 using the Hubbard U correction, Comput. Mater. Sci. 217 (2023), https://doi.org/10.1016/j.commatsci.2022.111913.
[261] G.R. Schleder, A.C.M. Padilha, C.M. Acosta, M. Costa, A. Fazzio, From DFT to machine learning: recent approaches to materials science - a review, J. Phys. Mater. 2 (2019), https://doi.org/10.1088/2515-7639/ab084b.
[262] E.B. Isaacs, H. Shin, A. Annaberdiyev, C. Wolverton, L. Mitas, A. Benali, O. Heinonen, Assessing the Accuracy of Compound Formation Energies with Quantum Monte Carlo, 2022, https://doi.org/10.1103/PhysRevB.105.224110.
[263] R. Peverati, D.G. Truhlar, Exchange-correlation functional with good accuracy for both structural and energetic properties while depending only on the density and its gradient, J. Chem. Theor. Comput. 8 (2012) 2310–2319, https://doi.org/10.1021/ct3002656.
[264] L. Goerigk, S. Grimme, Double-hybrid density functionals, Wiley Interdiscip. Rev. Comput. Mol. Sci. 4 (2014) 576–600, https://doi.org/10.1002/wcms.1193.
[265] A.S. Rad, DFT study of hydrogen fluoride and sulfur trioxide interactions on the surface of Pt-decorated graphene, J. Theor. Appl. Phys. 10 (2016) 307–313, https://doi.org/10.1007/s40094-016-0230-z.
[266] M. Chandel, D. Moitra, P. Makkar, H. Sinha, H.S. Hora, N.N. Ghosh, Synthesis of multifunctional CuFe2O4-reduced graphene oxide nanocomposite: an efficient magnetically separable catalyst as well as high performance supercapacitor and first-principles calculations of its electronic structures, RSC Adv. 8 (2018) 27725–27739, https://doi.org/10.1039/c8ra05393f.
[267] A.E. Torres, R. Flores, L. Fomina, S. Fomine, Electronic structure of boron-doped finite graphene sheets: unrestricted DFT and complete active space calculations, Mol. Simulat. 42 (2016) 1512–1518, https://doi.org/10.1080/08927022.2016.1214955.
[268] R.M. Torres-Rojas, D.A. Contreras-Solorio, L. Hernández, A. Enciso, Band gap variation in bi, tri and few-layered 2D graphene/hBN heterostructures, Solid State Commun. 341 (2022), https://doi.org/10.1016/j.ssc.2021.114553.
[269] N. Yuksel, A. Kose, M.F. Fellah, Sensing properties of propylene oxide on Pt and Pd doped graphene sheets: a DFT Investigation, Sens. Actuat. A Phys. 344 (2022), https://doi.org/10.1016/j.sna.2022.113726.
[270] P. Ziesche, S. Kurth, J.P. Perdew, Density Functionals from LDA to GGA, 1998.
[271] F. Riggio, Y. Brun, D. Karevski, A. Faribault, J. Dubail, Gradient Corrections to the Local Density Approximation in the One-Dimensional Bose Gas, 2022, https://doi.org/10.1103/PhysRevA.106.053309.
[272] P. Ballone, G. Galli, Accurate Pseudopotential Local-Density-Approximation Computations for Neutral and Ionized Dimers of the IB and IIB Groups, 1990.
[273] K.C. Wasalathilake, G.A. Ayoko, C. Yan, Effects of heteroatom doping on the performance of graphene in sodium-ion batteries: a density functional theory investigation, Carbon 140 (2018) 276–285, https://doi.org/10.1016/j.carbon.2018.08.071.
[274] J. Contreras-García, W. Yang, E.R. Johnson, Analysis of hydrogen-bond interaction potentials from the electron density: integration of noncovalent interaction regions, J. Phys. Chem. A 115 (2011) 12983–12990, https://doi.org/10.1021/jp204278k.
[275] M. Manadé, F. Viñes, F. Illas, Transition metal adatoms on graphene: a systematic density functional study, Carbon 95 (2015) 525–534, https://doi.org/10.1016/j.carbon.2015.08.072.
[276] A. Patra, B. Patra, L.A. Constantin, P. Samal, Electronic band structure of layers within meta generalized gradient approximation of density functionals, Phys. Rev. B 102 (2020), https://doi.org/10.1103/PhysRevB.102.045135.

[277] J. Heyd, G.E. Scuseria, M. Ernzerhof, Hybrid functionals based on a screened Coulomb potential, J. Chem. Phys. 118 (2003) 8207–8215, https://doi.org/10.1063/1.1564060.
[278] N. Kheirabadi, A. Shafiekhani, The ground state of graphene and graphene disordered by vacancies, Phys. E Low Dimens. Syst. Nanostruct. 47 (2013) 309–315, https://doi.org/10.1016/j.physe.2012.09.022.
[279] F. Opoku, K.K. Govender, C.G.C.E. van Sittert, P.P. Govender, Understanding the mechanism of enhanced charge separation and visible light photocatalytic activity of modified wurtzite ZnO with nanoclusters of ZnS and graphene oxide: from a hybrid density functional study, New J. Chem. 41 (2017) 8140–8155, https://doi.org/10.1039/c7nj01942d.
[280] R. Takassa, O. Farkad, E.A. Ibnouelghazi, D. Abouelaoualim, Electronic and optical properties of ultra-small diameter armchair carbon and boron nitride nanotubes by PBE, TB-mBJ and YS-PBE0 functionals, Diam. Relat. Mater. 123 (2022), https://doi.org/10.1016/j.diamond.2022.108863.
[281] D. Shiojiri, T. Iida, M. Yamaguchi, N. Hirayama, Y. Imai, Performance comparison of hybrid functionals for describing narrow-gap semiconductors: a study on low-temperature thermoelectric material α-SrSi2, Comput. Condens. Matter 30 (2022), https://doi.org/10.1016/j.cocom.2021.e00620.
[282] A. Karton, π–π interactions between benzene and graphene by means of large-scale DFT-D4 calculations, Chem. Phys. 561 (2022), https://doi.org/10.1016/j.chemphys.2022.111606.
[283] J.W. Furness, A.D. Kaplan, J. Ning, J.P. Perdew, J. Sun, Construction of Meta-GGA Functionals through Restoration of Exact Constraint Adherence to Regularized SCAN Functionals, 2021, https://doi.org/10.1063/5.0073623.
[284] V. v Karasiev, D.I. Mihaylov, S.X. Hu, Meta-GGa exchanGe-Correlation Free enerGy Density Functional to Increase the Accuracy oF WarM-Dense-Matter siMulations, n.d.
[285] M. Bursch, J.-M. Mewes, A. Hansen, S. Grimme, Best-Practice DFT Protocols for Basic Molecular Computational Chemistry**, 2022, https://doi.org/10.26434/chemrxiv-2022-n304h.
[286] A. Tarnopolsky, A. Karton, R. Sertchook, D. Vuzman, J.M.L. Martin, Double-hybrid functional for thermochemical kinetics, J. Phys. Chem. A 112 (2008) 3–8, https://doi.org/10.1021/jp710179r.
[297] S. Mohr, L.E. Ratcliff, L. Genovese, D. Caliste, P. Boulanger, S. Goedecker, T. Deutsch, Accurate and efficient linear scaling DFT calculations with universal applicability, Phys. Chem. Chem. Phys. 17 (2015) 31360–31370, https://doi.org/10.1039/c5cp00437c.
[298] J. Li, H.P.C. Miranda, Y.-M. Niquet, L. Genovese, I. Duchemin, L. Wirtz, C. Delerue, Phonon-limited Carrier Mobility and Resistivity from Carbon Nanotubes to Graphene, 2015, https://doi.org/10.1103/PhysRevB.92.075414.
[299] M.S. Sharif Azadeh, A. Kokabi, M. Hosseini, M. Fardmanesh, Tunable Bandgap Opening in the Proposed Structure of Silicon Doped Graphene, n.d.
[300] F. Ostovari, M. Hasanpoori, M. Abbasnejad, M.A. Salehi, DFT calculations of graphene monolayer in presence of Fe dopant and vacancy, Phys. B Condens. Matter 541 (2018) 6–13, https://doi.org/10.1016/j.physb.2018.04.023.
[301] J.H. Warner, Y.C. Lin, K. He, M. Koshino, K. Suenaga, Stability and spectroscopy of single nitrogen dopants in graphene at elevated temperatures, ACS Nano 8 (2014) 11806–11815, https://doi.org/10.1021/nn5054798.
[302] E. Şaşıoğlu, H. Hadipour, C. Friedrich, S. Blügel, I. Mertig, Strength of effective Coulomb interactions and origin of ferromagnetism in hydrogenated graphene, Phys. Rev. B 95 (2017), https://doi.org/10.1103/PhysRevB.95.060408.
[303] M. Rösner, E. Şaşıoğlu, C. Friedrich, S. Blügel, T.O. Wehling, Wannier Function Approach to Realistic Coulomb Interactions in Layered Materials and Heterostructures, 2015, https://doi.org/10.1103/PhysRevB.92.085102.
[304] S. Irmer, T. Frank, S. Putz, M. Gmitra, D. Kochan, J. Fabian, Spin-orbit Coupling in Fluorinated Graphene, 2014, https://doi.org/10.1103/PhysRevB.91.115141.
[305] R. Bhandari, V.K. Jindal, P. Rani, V.K. Jindal, Band Gap Modulation of Graphene with Increasing Concentration of Li/B Doping, n.d. https://www.researchgate.net/publication/275649449.
[306] N.M. Khatir, H. Fatoorehchi, A. Ahmadi, A. Khoshnoodfar, M. Faghihnasiri, Investigating the adsorption of the thyroid stimulating hormones molecules on graphene sheets by the density functional theory for possible nano-biosensor applications, J. Chem. Pet. Eng. 55 (2021) 385–392, https://doi.org/10.22059/JCHPE.2021.305285.1319.
[307] R. Das, N. Dhar, A. Bandyopadhyay, D. Jana, Size dependent magnetic and optical properties in diamond shaped graphene quantum dots: a DFT study, J. Phys. Chem. Solid. 99 (2016) 34–42, https://doi.org/10.1016/j.jpcs.2016.08.004.
[308] S.A. Jafari, M. Jahanshahi, M.G. Ahangari, Platinum adsorption onto graphene and oxidized graphene: a quantum mechanics study, Mater. Chem. Phys. 190 (2017) 17–24, https://doi.org/10.1016/j.matchemphys.2016.12.076.
[309] M.D. Moghaddam, S. Jamehbozorgi, M. Rezvani, V. Izadkhah, M.T. Moghim, Theoretical treatment of interaction of pyrazinamide with graphene and h-SiC monolayer: a DFT-D3 study, Phys. E Low Dimens. Syst. Nanostruct. 138 (2022), https://doi.org/10.1016/j.physe.2021.115077.
[310] S.S. Sadeghi, H. Simchi, Raman Spectra and Infrared Intensities of Graphene-like Clusters in Compared to Epitaxial Graphene on SiC, n.d.
[311] İ. Demiroğlu, Y. Karaaslan, T. Kocabaş, M. Keçeli, Á. Vázquez-Mayagoitia, C. Sevik, Computation of the thermal expansion coefficient of graphene with Gaussian approximation potentials, J. Phys. Chem. C 125 (2021) 14409–14415, https://doi.org/10.1021/acs.jpcc.1c01888.
[312] M. Campetella, N.M. Nguyen, J. Baima, L. Maschio, F. Mauri, M. Calandra, Hybrid-functional Electronic Structure of Multilayer Graphene, 2020, https://doi.org/10.1103/PhysRevB.101.165437.
[313] M.J. Cheng, M. Head-Gordon, A.T. Bell, How to chemically tailor metal-porphyrin-like active sites on carbon nanotubes and graphene for minimal overpotential in the electrochemical oxygen evolution and oxygen reduction reactions, J. Phys. Chem. C 118 (2014) 29482–29491, https://doi.org/10.1021/jp507638v.
[314] D. Cortes-Arriagada, L. Sanhueza, A. Bautista-Hernandez, M. Salazar-Villanueva, E. Chigo Anota, Chemical and physical viewpoints about the bonding in fullerene-graphene hybrid materials: interaction on pristine and Fe-doped graphene, J. Phys. Chem. C 123 (2019) 24209–24219, https://doi.org/10.1021/acs.jpcc.9b07702.
[315] D. Le, A. Kara, E. Schröder, P. Hyldgaard, T.S. Rahman, Physisorption of nucleobases on graphene: a comparative van der Waals study, J. Phys. Condens. Matter 24 (2012), https://doi.org/10.1088/0953-8984/24/42/424210.
[316] M. Vanin, J.J. Mortensen, A.K. Kelkkanen, J.M. Garcia-Lastra, K.S. Thygesen, K.W. Jacobsen, Graphene on metals: a Van der Waals density functional study, 2009, https://doi.org/10.1103/PhysRevB.81.081408.
[317] J.P. Perdew, Jacob's Ladder of Density Functional Approximations for the Exchange-Correlation Energy, AIP Publishing, 2003, pp. 1–20, https://doi.org/10.1063/1.1390175.
[318] Q. Peng, F. Duarte, R.S. Paton, Computing organic stereoselectivity-from concepts to quantitative calculations and predictions, Chem. Soc. Rev. 45 (2016) 6093–6107, https://doi.org/10.1039/c6cs00573j.
[319] M.P. McBee, O.A. Awan, A.T. Colucci, C.W. Ghobadi, N. Kadom, A.P. Kansagra, S. Tridandapani, W.F. Auffermann, Deep learning in radiology, Acad. Radiol. 25 (2018) 1472–1480, https://doi.org/10.1016/j.acra.2018.02.018.
[320] A. Chandrasekaran, D. Kamal, R. Batra, C. Kim, L. Chen, R. Ramprasad, Solving the electronic structure problem with machine learning, NPJ Comput Mater 5 (2019), https://doi.org/10.1038/s41524-019-0162-7.
[321] G.R. Schleder, A.C.M. Padilha, C.M. Acosta, M. Costa, A. Fazzio, From DFT to machine learning: recent approaches to materials science - a review, J. Phys. Mater. 2 (2019), https://doi.org/10.1088/2515-7639/ab084b.
[322] J. Behler, Four generations of high-dimensional neural network potentials, Chem. Rev. 121 (2021) 10037–10072, https://doi.org/10.1021/acs.chemrev.0c00868.
[323] H.J. Kulik, T. Hammerschmidt, J. Schmidt, S. Botti, M.A.L. Marques, M. Boley, M. Scheffler, M. Todorović, P. Rinke, C. Oses, A. Smolyanyuk, S. Curtarolo, A. Tkatchenko, A.P. Bartók, S. Manzhos, M. Ihara, T. Carrington, J. Behler, O. Isayev, M. Veit, A. Grisafi, J. Nigam, M. Ceriotti, K.T. Schütt, J. Westermayr, M. Gastegger, R.J. Maurer, B. Kalita, K. Burke, R. Nagai, R. Akashi, O. Sugino, J. Hermann, F. Noé, S. Pilati, C. Draxl, M. Kuban, S. Rigamonti, M. Scheidgen, M. Esters, D. Hicks, C. Toher, P.v. Balachandran, I. Tamblyn, S. Whitelam, C. Bellinger, L.M. Ghiringhelli, Roadmap on Machine learning in electronic structure, Electron. Struct. 4 (2022), https://doi.org/10.1088/2516-1075/ac572f.

[324] H. Li, Z. Wang, N. Zou, M. Ye, R. Xu, X. Gong, W. Duan, Y. Xu, Deep-Learning Density Functional Theory Hamiltonian for Efficient Ab Initio Electronic-Structure Calculation, 2021, https://doi.org/10.1038/s43588-022-00265-6.
[325] P. Friederich, F. Häse, J. Proppe, A. Aspuru-Guzik, Machine-learned potentials for next-generation matter simulations, Nat. Mater. 20 (2021) 750–761, https://doi.org/10.1038/s41563-020-0777-6.
[326] P.G.D.E.G. Designed Research; T, P.M.P.E.G. Performed Research; T, Signatures of a Liquid-Liquid Transition in an Ab Initio Deep Neural Network Model for Water, 117, 2020, pp. 26040–26046, https://doi.org/10.1073/pnas.2015440117/-/DCSupplemental.
[327] K.T. Schütt, H.E. Sauceda, P.-J. Kindermans, A. Tkatchenko, K.-R. Müller, SchNet - a Deep Learning Architecture for Molecules and Materials, 2017, https://doi.org/10.1063/1.5019779.
[328] L. Zhang, J. Han, H. Wang, R. Car, E. Weinan, Deep potential molecular dynamics: a scalable model with the accuracy of quantum mechanics, Phys. Rev. Lett. 120 (2018), https://doi.org/10.1103/PhysRevLett.120.143001.
[329] F. Brockherde, L. Vogt, L. Li, M.E. Tuckerman, K. Burke, K.R. Müller, Bypassing the Kohn-Sham equations with machine learning, Nat. Commun. 8 (2017), https://doi.org/10.1038/s41467-017-00839-3.
[330] T.T. Nguyen, E. Székely, G. Imbalzano, J. Behler, G. Csányi, M. Ceriotti, A.W. Götz, F. Paesani, Comparison of Permutationally Invariant Polynomials, Neural Networks, and Gaussian Approximation Potentials in Representing Water Interactions through Many-Body Expansions, 2018, https://doi.org/10.1063/1.5024577.
[331] A.P. Bartõk, G. Csányi, Gaussian approximation potentials: a brief tutorial introduction, Int. J. Quant. Chem. 115 (2015) 1051–1057, https://doi.org/10.1002/qua.24927.
[332] S. Attarian, D. Morgan, I. Szlufarska, Thermophysical properties of FLiBe using moment tensor potentials, J. Mol. Liq. (2022), 120803, https://doi.org/10.1016/j.molliq.2022.120803.
[333] I.I. Novoselov, A.v. Yanilkin, A.v. Shapeev, E.v. Podryabinkin, Moment tensor potentials as a promising tool to study diffusion processes, Comput. Mater. Sci. 164 (2019) 46–56, https://doi.org/10.1016/j.commatsci.2019.03.049.
[334] Y. Zhang, J. Duchi, M. Wainwright, Divide and Conquer Kernel Ridge Regression: A Distributed Algorithm with Minimax Optimal Rates, 2015.
[335] P. Exterkate, P.J.F. Groenen, C. Heij, D. van Dijk, Nonlinear forecasting with many predictors using kernel ridge regression, Int. J. Forecast. 32 (2016) 736–753, https://doi.org/10.1016/j.ijforecast.2015.11.017.
[336] K. Yao, J.E. Herr, D.W. Toth, R. McKintyre, J. Parkhill, The TensorMol-0.1 model chemistry: a neural network augmented with long-range physics, Chem. Sci. 9 (2018) 2261–2269, https://doi.org/10.1039/c7sc04934j.
[337] R. Lot, F. Pellegrini, Y. Shaidu, E. Küçükbenli, PANNA: properties from artificial neural network architectures, Comput. Phys. Commun. 256 (2020), 107402, https://doi.org/10.17632/mcryj6cnnh.1.
[338] P. Pattnaik, S. Raghunathan, T. Kalluri, P. Bhimalapuram, C.v. Jawahar, U. Deva Priyakumar, Machine learning for accurate force calculations in molecular dynamics simulations, J. Phys. Chem. A 124 (2020) 6954–6967, https://doi.org/10.1021/acs.jpca.0c03926.
[339] A.P. Thompson, L.P. Swiler, C.R. Trott, S.M. Foiles, G.J. Tucker, Spectral neighbor analysis method for automated generation of quantum-accurate interatomic potentials, J. Comput. Phys. 285 (2015) 316–330, https://doi.org/10.1016/j.jcp.2014.12.018.
[340] S. Venturi, R.L. Jaffe, M. Panesi, Bayesian machine learning approach to the quantification of uncertainties on ab initio potential energy surfaces, J. Phys. Chem. A 124 (2020) 5129–5146, https://doi.org/10.1021/acs.jpca.0c02395.
[341] L.J. Butler, Chemical Reaction Dynamics Beyond the Born-oppenheimer Approximation, 1998.
[342] J. Flick, M. Ruggenthaler, H. Appel, A. Rubio, Atoms and molecules in cavities, from weak to strong coupling in quantum-electrodynamics (QED) chemistry, Proc. Natl. Acad. Sci. U. S. A. 114 (2017) 3026–3034, https://doi.org/10.1073/pnas.1615509114.
[343] J. Behler, Four generations of high-dimensional neural network potentials, Chem. Rev. 121 (2021) 10037–10072, https://doi.org/10.1021/acs.chemrev.0c00868.
[344] P. Rowe, G. Csányi, D. Alfè, A. Michaelides, A Machine Learning Potential for Graphene, 2017, https://doi.org/10.1103/PhysRevB.97.054303.
[345] P. Pattnaik, S. Raghunathan, T. Kalluri, P. Bhimalapuram, C. v Jawahar, U. Deva Priyakumar, Machine Learning for Accurate Force Calculations in Molecular Dynamics Simulations, n.d.
[346] T.W. Ko, J.A. Finkler, S. Goedecker, J. Behler, A fourth-generation high-dimensional neural network potential with accurate electrostatics including non-local charge transfer, Nat. Commun. 12 (2021), https://doi.org/10.1038/s41467-020-20427-2.
[347] H. Huo, M. Rupp, Unified representation of molecules and crystals for machine learning, Mach. Learn. Sci. Technol. (2022), https://doi.org/10.1088/2632-2153/aca005.
[348] C. van der Oord, G. Dusson, G. Csányi, C. Ortner, Regularised atomic body-ordered permutation-invariant polynomials for the construction of interatomic potentials, Mach. Learn. Sci. Technol. 1 (2020), https://doi.org/10.1088/2632-2153/ab527c.
[349] O.A. von Lilienfeld, R. Ramakrishnan, M. Rupp, A. Knoll, Fourier Series of Atomic Radial Distribution Functions: A Molecular Fingerprint for Machine Learning Models of Quantum Chemical Properties, 2013. http://arxiv.org/abs/1307.2918.
[350] J. Behler, Perspective: machine learning potentials for atomistic simulations, J. Chem. Phys. 145 (2016), https://doi.org/10.1063/1.4966192.
[351] A. Mannodi-Kanakkithodi, G. Pilania, T.D. Huan, T. Lookman, R. Ramprasad, Machine learning strategy for accelerated design of polymer dielectrics, Sci. Rep. 6 (2016), https://doi.org/10.1038/srep20952.
[352] R. Ramprasad, R. Batra, G. Pilania, A. Mannodi-Kanakkithodi, C. Kim, Machine learning in materials informatics: recent applications and prospects, NPJ Comput. Mater. 3 (2017), https://doi.org/10.1038/s41524-017-0056-5.
[353] M. Dou, M. Fyta, Lithium adsorption on 2D transition metal dichalcogenides: towards a descriptor for machine learned materials design, J. Mater. Chem. A Mater. 8 (2020) 23511–23518, https://doi.org/10.1039/d0ta04834h.
[354] W. Zhang, W. Huang, J. Tan, Q. Guo, B. Wu, Heterogeneous catalysis mediated by light, electricity and enzyme via machine learning: paradigms, applications and prospects, Chemosphere 308 (2022), https://doi.org/10.1016/j.chemosphere.2022.136447.
[355] P. Pentyala, V. Singhania, V.K. Duggineni, P.A. Deshpande, Machine learning-assisted DFT reveals key descriptors governing the vacancy formation energy in Pd-substituted multicomponent ceria, Mol. Catal. 522 (2022), https://doi.org/10.1016/j.mcat.2022.112190.
[356] F. Cailliez, P. Pernot, Statistical approaches to forcefield calibration and prediction uncertainty in molecular simulation, J. Chem. Phys. 134 (2011), https://doi.org/10.1063/1.3545069.
[357] P. Angelikopoulos, C. Papadimitriou, P. Koumoutsakos, Bayesian uncertainty quantification and propagation in molecular dynamics simulations: a high performance computing framework, J. Chem. Phys. 137 (2012), https://doi.org/10.1063/1.4757266.
[358] R.A. Messerly, T.A. Knotts, W.V. Wilding, Uncertainty quantification and propagation of errors of the Lennard-Jones 12-6 parameters for n-alkanes, J. Chem. Phys. 146 (2017), https://doi.org/10.1063/1.4983406.
[359] M. Wen, E.B. Tadmor, Uncertainty quantification in molecular simulations with dropout neural network potentials, NPJ Comput. Mater. 6 (2020), https://doi.org/10.1038/s41524-020-00390-8.
[360] R. Ramprasad, R. Batra, G. Pilania, A. Mannodi-Kanakkithodi, C. Kim, Machine learning in materials informatics: recent applications and prospects, NPJ Comput. Mater. 3 (2017), https://doi.org/10.1038/s41524-017-0056-5.
[361] T. Hastie, R. Tibshirani, J. Friedman, Springer Series in Statistics the Elements of Statistical Learning Data Mining, Inference, and Prediction, n.d.
[362] A.G. Wilson, The Case for Bayesian Deep Learning, 2020. http://arxiv.org/abs/2001.10995.
[363] S. Fathololoumi, A.R. Vaezi, S.K. Alavipanah, A. Ghorbani, A. Biswas, Comparison of spectral and spatial-based approaches for mapping the local variation of soil moisture in a semi-arid mountainous area, Sci. Total Environ. (2020) 724, https://doi.org/10.1016/j.scitotenv.2020.138319.
[364] Z. Yang, W. Gao, Applications of machine learning in alloy catalysts: rational selection and future development of descriptors, Adv. Sci. 9 (2022), https://doi.org/10.1002/advs.202106043.
[365] Z. Ghahramani, Unsupervised learning *. http://www.gatsby.ucl.ac.uk/~zoubin, 2004.
[366] X. Zhu, Z. Ghahramani, J. Lafferty, Semi-Supervised Learning Using Gaussian Fields and Harmonic Functions, n.d.

[367] G. Taranto-Vera, P. Galindo-Villardón, J. Merchán-Sánchez-Jara, J. Salazar-Pozo, A. Moreno-Salazar, V. Salazar-Villalva, Algorithms and software for data mining and machine learning: a critical comparative view from a systematic review of the literature, J. Supercomput. 77 (2021) 11481–11513, https://doi.org/10.1007/s11227-021-03708-5.
[368] J. Desloires, D. Ienco, A. Botrel, N. Ranc, Positive unlabelled learning for satellite images'time series analysis: an application to cereal and forest mapping, Rem. Sens. 14 (2022), https://doi.org/10.3390/rs14010140.
[369] I.S. Novikov, K. Gubaev, E. v Podryabinkin, A. v Shapeev, The MLIP package: moment tensor potentials with MPI and active learning, Mach. Learn. Sci. Technol. 2 (2021), 025002, https://doi.org/10.1088/2632-2153/abc9fe.
[370] M. Babar, H.L. Parks, G. Houchins, V. Viswanathan, An accurate machine learning calculator for the lithium-graphite system, J. Phys. Energy 3 (2021), https://doi.org/10.1088/2515-7655/abc96f.
[371] Z. Yang, W. Gao, Applications of machine learning in alloy catalysts: rational selection and future development of descriptors, Adv. Sci. 9 (2022), https://doi.org/10.1002/advs.202106043.
[372] G.P.P. Pun, R. Batra, R. Ramprasad, Y. Mishin, Physically informed artificial neural networks for atomistic modeling of materials, Nat. Commun. 10 (2019), https://doi.org/10.1038/s41467-019-10343-5.
[373] M. Tang, Q. Song, N. Li, Z. Jiang, R. Huang, G. Cheng, Enhancement of electrical signaling in neural networks on graphene films, Biomaterials 34 (2013) 6402–6411, https://doi.org/10.1016/j.biomaterials.2013.05.024.
[374] C. Zhang, Q. Sun, Gaussian approximation potential for studying the thermal conductivity of silicene, J. Appl. Phys. 126 (2019), https://doi.org/10.1063/1.5119281.
[375] Y. Chen, J. Zhu, Y. Xie, N. Feng, Q.H. Liu, Smart inverse design of graphene-based photonic metamaterials by an adaptive artificial neural network, Nanoscale 11 (2019) 9749–9755, https://doi.org/10.1039/c9nr01315f.
[376] L. Shen, Y. Wang, W. Lai, Development of a machine learning potential for the study of crack propagation in titanium, Int. J. Pres. Ves. Pip. 194 (2021), https://doi.org/10.1016/j.ijpvp.2021.104514.
[377] Y. Shaidu, E. Küçükbenli, R. Lot, F. Pellegrini, E. Kaxiras, S. de Gironcoli, A systematic approach to generating accurate neural network potentials: the case of carbon, NPJ Comput. Mater. 7 (2021), https://doi.org/10.1038/s41524-021-00508-6.
[378] S. Fujikake, V.L. Deringer, T.H. Lee, M. Krynski, S.R. Elliott, G. Csányi, Gaussian Approximation Potential Modeling of Lithium Intercalation in Carbon Nanostructures, 2017, https://doi.org/10.1063/1.5016317.
[379] M. Wen, E.B. Tadmor, Hybrid neural network potential for multilayer graphene, Phys. Rev. B 100 (2019), https://doi.org/10.1103/PhysRevB.100.195419.
[380] C. León, R. Melnik, Studies of Shape Memory Graphene Nanostructures via Integration of Physics-Based Modelling and Machine Learning, n.d.
[381] B. Mortazavi, I.S. Novikov, E.v. Podryabinkin, S. Roche, T. Rabczuk, A.v. Shapeev, X. Zhuang, Exploring phononic properties of two-dimensional materials using machine learning interatomic potentials, Appl. Mater. Today 20 (2020), https://doi.org/10.1016/j.apmt.2020.100685.
[382] J. Klimeš, A. Michaelides, Perspective: advances and challenges in treating van der Waals dispersion forces in density functional theory, J. Chem. Phys. 137 (2012), https://doi.org/10.1063/1.4754130.
[383] V. Shukla, Y. Jiao, J.-H. Lee, E. Schroder, J.B. Neaton, P. Hyldgaard, Accurate non-empirical range-separated hybrid van der Waals density functional for complex molecular problems, solids, and surfaces, 2022, https://doi.org/10.1103/PhysRevX.12.041003.
[384] X. Gu, Z. Fan, H. Bao, C.Y. Zhao, Revisiting phonon-phonon scattering in single-layer graphene, Phys. Rev. B 100 (2019), https://doi.org/10.1103/PhysRevB.100.064306.
[385] A.N. Toksumakov, G.A. Ermolaev, M.K. Tatmyshevskiy, Y.A. Klishin, A.S. Slavich, I.v. Begichev, D. Stosic, D.I. Yakubovsky, D.G. Kvashnin, A.A. Vyshnevyy, A. v. Arsenin, V.S. Volkov, D.A. Ghazaryan, Anomalous optical response of graphene on hexagonal boron nitride substrates, Commun. Phys. 6 (2023) 13, https://doi.org/10.1038/s42005-023-01129-9.
[386] X. Chen, F. Wang, Q. Gu, J. Yang, M. Yu, D. Kwong, C.W. Wong, H. Yang, H. Zhou, S. Zhou, Multifunctional optoelectronic device based on graphene-coupled silicon photonic crystal cavities, Opt. Express 29 (2021), 11094, https://doi.org/10.1364/oe.421596.
[387] M. Gao, Q.-Z. Li, X.-W. Yan, J. Wang, Prediction of Phonon-Mediated Superconductivity in Borophene, 2016, https://doi.org/10.1103/PhysRevB.95.024505.
[388] M. Ostermann, P. Velicsanyi, P. Bilotto, J. Schodl, M. Nadlinger, G. Fafilek, P.A. Lieberzeit, M. Valtiner, Development and up-scaling of electrochemical production and mild thermal reduction of graphene oxide, Materials 15 (2022), https://doi.org/10.3390/ma15134639.
[389] Q. Cao, X. Geng, H. Wang, P. Wang, A. Liu, Y. Lan, Q. Peng, A review of current development of graphene mechanics, Crystals 8 (2018), https://doi.org/10.3390/cryst8090357.